

## ABSTRACT

Title of Thesis: LOWER-BODY MECHANICAL  
PERTURBATION OF GAIT TO IDENTIFY  
NEURAL CONTROL

*Shakiba Rafiee, Master of Arts, 2017*

Thesis Directed By: Professor Tim Kiemel,  
Department of Kinesiology

Neural feedback plays a key role in maintaining locomotor stability in face of perturbations. In this study, we systematically identified properties of neural feedback that contribute to stabilizing human walking by examining how the nervous system responds to small kinematic deviations away from the desired gait pattern. We applied small continuous mechanical perturbation, forces at the ankles, as well as small continuous sensory perturbation, movement of a virtual visual scene, in order to compare how neural feedback responds to actual and illusory kinematic deviations. Computing phase-dependent impulse response functions ( $\phi$ IRFs) that describe kinematic and muscular responses to small brief perturbations (impulses), enabled us to identify critical phases of the gait cycle when the nervous system modulates muscle activity. In particular, our results suggest that an early-stance modulation of anterior leg-muscles is a general control mechanism that serves multiple functions, including controlling walking speed and compensating for errors in foot placement.

LOWER-BODY MECHANICAL PERTURBATION OF GAIT TO  
IDENTIFY NEURAL CONTROL

by

Shakiba Rafiee

Thesis submitted to the Faculty of the Graduate School of the  
University of Maryland, College Park, in partial fulfillment  
of the requirements for the degree of  
Master of Arts  
2017

Advisory Committee:  
Professor Tim Kiemel, Chair  
Professor Ross H. Miller  
Professor Jae Kun Shim

© Copyright by  
Shakiba Rafiee  
2017

## Acknowledgment

I would like to first thank my advisor, Tim Kiemel, without whom this work would have not been possible. Thank you for giving me the opportunity to work at the “cognitive motor neuroscience” lab, for teaching me signal processing, and for making my transition to motor control studies easier. Thank you for keeping an open door at all time and for the discussions that shaped my understanding of neural control.

My special thanks also go to my dissertation committee, Ross Miller, and Jae Kun Shim, whose feedback helped improve this study and thought me the importance of critical thinking.

Finally, I would like to thank my parents, Farideh and Reza. Nothing would have been possible without you, your support, your patience and your love. I am so blessed to have you in my life. Thank you.

# Table of Contents

Chapter 1 : Introduction .....	1
Background .....	1
Neural Control of Human Balance (Posture and Gait) .....	1
Stability .....	2
Research Question .....	4
Suggested Solution.....	5
How to Study Deviations in the System .....	5
How to Quantify the System Responses to the Perturbations?.....	6
Specific aims .....	7
Chapter 2 : Literature Review .....	9
What is known about neural control of locomotion from physiological studies? .....	9
Evidence of Anticipatory Control of Locomotion .....	10
Evidence of Reactive Control of Locomotion .....	11
Stabilizing Mechanisms in Neuromechanical Models .....	11
Reactive Control Models .....	12
Models with Anticipatory Control .....	14
A Model with both Anticipatory and Reactive Control .....	15
What is known about the control based on experimental data? .....	15
Chapter 3 : Methods .....	17
Subjects .....	17
Procedure .....	17
Protocol .....	17
Data collection .....	19
Data Analysis .....	20
Signal Processing .....	20
System Identification .....	20
Statistics .....	26
Chapter 4 : Results .....	27
Mechanical Perturbation .....	27
Phase Response to Mechanical Perturbations .....	27
Kinematic Responses to Mechanical Perturbations .....	28
EMG Responses to the Mechanical Perturbation .....	33
Sensory Perturbation .....	37

Phase Response to Sensory Perturbations.....	38
EMG Responses to Sensory Perturbations .....	38
Kinematic Responses to Sensory Perturbations.....	41
Comparing Perturbed and Unperturbed Mean Waveforms .....	42
Chapter 5 : Discussion .....	45
Open-loop Responses.....	46
Feedback Responses .....	47
Conclusion .....	49
Future Directions .....	50
Appendixes .....	51
Appendix A: Symmetry .....	51
Appendix B: Mass-Spring-Damper System Impulse Response .....	52
Bibliography .....	53

## Chapter 1 : Introduction

### Background

Walking seems like an easy task; we do not need to think as we walk in order to stabilize ourselves. However, just comparing this reality with the troubles that the roboticists go through to achieve dynamic stability in biped robots (i.e. providing the system with fast feedback and high elasticity) shows that the challenges are real. Human locomotion is a complex rhythmic movement. One of its important aspects is the ability of the system to stabilize in the face of continual small perturbations that arise from both internal (e.g., neuromuscular and sensory noise) and external sources (e.g., variation in walking surfaces or changes in optic flow). There are several models of human walking that seek to put together the pieces of information that we have acquired about the control strategies used in walking. However, there is little information on the specifics of the control strategies that the nervous system adopts to correct for small “subtle” perturbations and on the role of sensory feedback in those strategies. In this study, we seek to answer aspects of these questions.

### Neural Control of Human Balance (Posture and Gait)

The neural control of human balance is the result of the interaction of two systems: 1) the musculoskeletal system, which is responsible for producing movement and 2) the nervous system which dictates the neural command. These systems work with each other in order to maintain balance, and they operate via two main groups of control mechanisms: passive mechanisms and active ones. The passive control mechanisms (or reflexes) exist at the lowest end of neuromechanical hierarchy [Holmes et al., 2006]. These strategies are driven by the viscoelastic properties of muscles and as a result there is no delay in the response produced by passive strategies. On the other hand, the active control strategies are mediated by the nervous system; therefore, there is a delay in the response produced by active strategies. Sensory information is essential in coordinating the muscle activations required for stabilizing the body in both postural and locomotor control. The human body during upright stance and walking is inherently unstable in the absence of neural feedback. However, the mechanisms that use sensory information to ensure stability are only partially known. In this study, we seek to better understand the role of sensory information in gait stability.

From a control theory perspective, the interactions between the musculoskeletal system and the nervous system that lead to movement can be described by a closed-

loop system that is composed of two main entities: 1) the plant, the entity being controlled; and 2) neural feedback, the entity that controls (Figure 1-1). The plant describes how the control signal (muscle activation as measured by EMG) causes movement, and neural feedback describes how movement causes execution of the

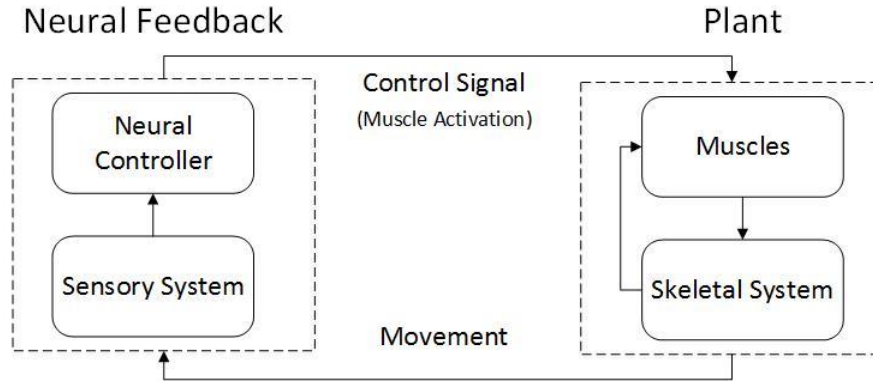


*Figure 1-1) Schematic diagram of the balance control.*

motor commands based on sensory inputs.

Our goal is to study stability in this closed loop system and to better understand the control strategies that the nervous system uses to stabilize human walking. More specifically, we want to know the mapping from movement to muscle activation in this closed loop system without opening the loop. That is because if we open the loop by removing the plant from the system and impose movement on the system with an external device (such as LOKOMAT [Jezernik et al., 2003]) there is no guarantee that the person would activate his/her muscles in a natural way.

### Stability

Stability is a concept that addresses the question of what will eventually happen in a system that has been perturbed. From a dynamical systems perspective (in the wider sense as a branch of mathematics), the state of a system at any point in time is a vector of values that contains all the information necessary to predict the system's future behavior [Guckenheimer and Holmes, 2013]. The system's state space is the set of all possible states. As time increases, the state of the system moves through state space along a trajectory. An ongoing observed behavior of a system corresponds to an attractor, a set of states toward which the system evolves in time. Such a behavior is necessarily stable, that is, the system returns to the behavior following any small



transient perturbation. Below we consider the attractor and stability for both posture and walking.

*Posture and Walking Stability*

Human standing posture can be usefully approximated as a linear time invariant (LTI) input-output system (e.g., [Peterka, 2000]), which mean that the relationship between a perturbation (the input) and any response variable (the output) is linear and the laws governing the system's dynamics do not depend on time. The attractor in this system corresponds to a *stable fixed point* in the state space (Figure 1-2A.) Since human posture is stable, after applying a small transient perturbation, the system comes back to the unperturbed position, the stable fixed point, and stays there. On the other hand, the attractor for walking can be idealized as a *stable limit cycle* (e.g., [Geyer and Herr, 2010; Pai and Patton, 1997; Taga et al., 1991]), a closed trajectory in state space (Figure 1-2C.) Since the limit cycle is stable, after applying a small transient perturbation, the system returns to the limit cycle. However, the perturbation will, in general, produce a lasting phase shift [Winfrey, 2001]. In the other words, following a small transient perturbation, the system returns to the original gait pattern but shifted slightly in time. A special case of stable gait is walking in sync with a metronome, which prevents a transient perturbation from producing a lasting phase shift. In this case, the system can be approximated as linear time period (LTP), which means that the system's dynamics

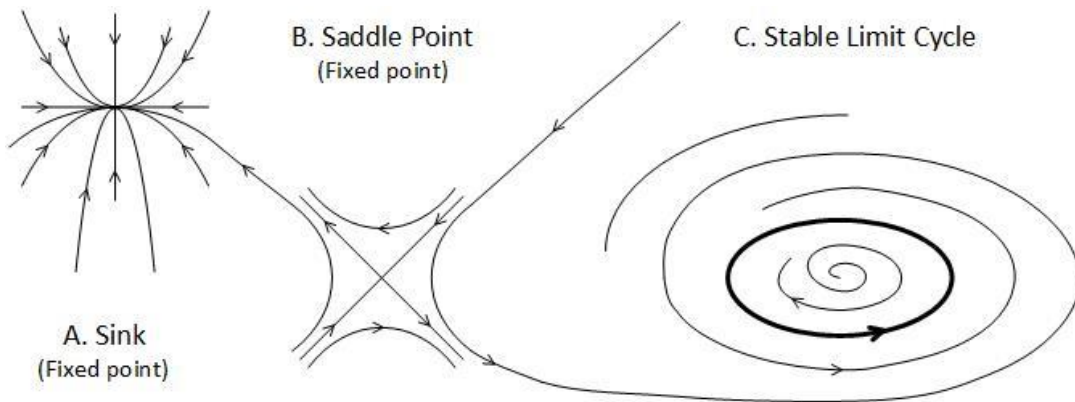


*Figure 1-2) Three type of attractors. A. Sink: an example of a stable fixed point in the phase space; it is a point into which all near trajectories flow in. B. Saddle point: a point that is stable only in one direction, C. Stable limit cycle (shown in bold): a loop toward which all neighboring trajectories flow*

are linear at each point in time, but change periodically with time [Möllerstedt and Bernhardsson, 2000; Wereley, 1990]

Several studies have addressed stability in human walking. Their main goal was to quantify stability using either: 1) variability measures (e.g. [Dingwell et al., 2001], [Terrier and Dériaz, 2011]), inspired by the notion that the natural fluctuations which occur during locomotion reflect local perturbations; or 2) measures directly related to the definition of stability, such as the maximum Floquet multiplier (e.g. Kang and Dingwell [2006]). Although these analyses provide insight into the stability of gait, they do not fully describe the neural control strategies that ensure stability. Consequently, it is evident that there exists a gap in our knowledge regarding the local stability of walking.

### Research Question

In this project, we are interested in studying local stability in human locomotion. We seek to find the control strategies our nervous system implements to maintain stability during walking. To this end, the system has to correct for perturbations that naturally occur to the system using some combination of passive (preflex) and active (reflex) control [Holmes et al., 2006]. Here, we are interested in the role of sensory information in active control strategies. Examples of such control strategies already exists in the postural control literature. Studying posture, Horak and Nashner [1986] found that in response to small perturbations the nervous system uses ankle muscles to rotate the upper and lower body in phase, while in response to larger perturbations it uses hip muscle to rotate the upper body out of phase with lower body. Later Creath et al. [2005] established that during unperturbed standing, an in-phase pattern between the lower and upper body at low frequencies co-exists with an anti-phase pattern at high frequencies.

In models of human walking, it is still debated what control strategies stabilize locomotion. The strategies responsible for gait stability may be similar to those responsible for postural stability. However, due to the rhythmic nature of human walking, the control strategies are expected to be phase-dependent. Examples of such suggested control strategies are prevalent in literature. One prevailing idea is that the control strategy is regulated by major gait events, i.e., heel strike and push-off. For example, both Kuo [2007] and Srinivasan and Ruina [2006] suggested simple models of locomotion that focus on the role of energy dissipation and regulate walking through sets of collisions (heel-strikes) and push-offs. Geyer et al. [2006] suggested a simple model of walking in which the locomotion was regulated by ensuring that the leg angle at heel strike is at some specified value, and Seipel and Holmes [2005] used a model

of locomotion that predominantly stabilized the system using feedback adjustments of leg angle at heel strike. Like the modeling literature, the experimental literature has also emphasized foot placement as an important determinant of gait stability. Using margin of stability, Hof [2008] found that foot placement could be used to enforce stability during walking. In general, in order to achieve stable walking, one must constantly adjust the timing and location of foot placement [Nashner, 1980]. However, little is known about the neural control strategies that regulates foot placement. O'Connor and Kuo [2009] have suggested that anterior-posterior (AP) balance during walking might be maintained with little “higher-level integrative” control, but rather through low-level propriospinal control strategies

In this study, we seek to understand foot placement strategies and the responses to deviations in foot placement. We want to find out if the nervous system predominantly regulates walking through push-offs and collisions. If the system is perturbed, will it wait until these time points to correct itself or will it respond at the first opportunity? The answer to these questions can help us find the mechanisms used in normal human walking. Logan et al. [2017] have previously used upper body mechanical perturbations to address this goal. In this study, we take an important next step by studying human walking responses to lower-body perturbations.

### Suggested Solution

As mentioned earlier, we are interested in identifying mechanisms that ensure local stability in human walking. That is to say, we want to find out how the controller responds to small kinematic deviations away from the desired gait pattern (limit cycle) by creating deviations in control signals (as measured by EMG). To do this, we must address how to study these deviations and how to quantify them.

#### How to Study Deviations in the System

To address local stability, we assume that the deviations in the system are small, yielding a local limit cycle (LLC) approximation of the system. Kinematic and EMG deviations in the system are either due to intrinsic perturbations such as motor or sensory noise or external factors. Therefore, historically, two main methods have been adopted to study local stability: 1) studying variability due to the system’s intrinsic perturbations; or 2) applying external perturbation and studying the system’s responses to these known perturbations. The first method is easier to conduct experimentally. However, using system’s intrinsic perturbations, it is difficult to determine which component of the closed-loop system has caused the deviations, since the intrinsic perturbations cannot be measured. On the other hand, using external perturbations,

system identification (ID) methods can be used to characterize the components of the dynamical system. As a result, we have decided to perturb the system externally in this study.

One other issue that needs to be addressed here is the nature of the perturbations (discrete or continuous). We know that the responses to external perturbations in walking are highly phase-dependent. In addition, we plan to use small perturbations to address local stability. If we were to use small discrete perturbations, we would need to apply perturbations at many different phases of the gait cycle to characterize phase dependence. For each phase of the gait cycle, we would need to apply the perturbation many times to separate out the effect of the perturbation from intrinsic gait variability. Finally, we would need to wait some amount of time between perturbations to allow the effect of one perturbation to decay before applying the next perturbation. As a result, the time required would probably not be experimentally feasible. Taking these considerations into account, continuous perturbation is the better option for this study.

The remaining question is how we want to perturb the system. Few studies have perturbed locomotion using continuous small mechanical perturbations [Logan et al., 2017; Moore et al., 2015]. Focusing on the importance of the trunk in balance control, Logan et al. [2017] perturbed walking mechanically at upper trunk. Computing the muscular and kinematic responses of the system to the perturbation signals, Logan et al. [2017] found indications of active neural control. In addition, their findings suggested that the nervous system stabilizes gait by modulating muscles activation during the phases of the gait when the muscles are normally active. (See the literature review section below for more information.)

In this study, we want to produce kinematic perturbations that potentially affect foot placement and investigate how neural feedback responds to such perturbations in order to either correct foot placement or compensate for deviations in foot placement. To achieve this goal, we will use a novel method to continuously perturb the legs by applying small forces at the ankles.

### How to Quantify the System Responses to the Perturbations?

The system will be perturbed using continuous mechanical and sensory perturbations. In order to characterize the muscular (from electromyographic signals) and kinematic responses to the perturbations, we will use harmonic transfer functions (HTFs). An HTF describes the input-output mapping for a LTP system [Möllerstedt and Bernhardsson, 2000]. In order to apply this method to limit-cycle systems (such as walking), the use of HTFs needs to be extended to account for the perturbations that reset the phase of the gait cycle [Kiemel et al., 2016; Logan et al., 2017]. Using the extended HTF method, we will characterize the system responses to the perturbations

in the frequency domain. The results will then be converted to the time (phase) domain to obtain phase-dependent impulse response functions ( $\phi$ IRFs). A  $\phi$ IRF describes the response of the system to a small brief perturbation (an impulse) at any phase of the gait cycle.

There are two approaches that can be used to infer open-loop properties based on closed-loop responses: joint input-output inference and short-latency inference [Kiemel et al., 2016]. Joint input-output inference is based on the fact that kinematic and muscular responses depend on both the plant and neural feedback, but the relationship between them only depends on one of them. For a mechanical perturbation, the relationship depends on neural feedback, and for a sensory perturbation it depends on the plant. In other words, for a mechanical perturbation neural feedback describes how kinematic responses cause muscular responses and for a sensory perturbation the plant explains how muscular responses cause kinematic responses. Whereas joint input-output inference uses responses to a mechanical perturbation to infer properties of neural feedback, short-latency inference uses responses to a sensory perturbation to infer properties of neural feedback and involves two limitations: (i) it is based on an assumption of how the sensory perturbation is related to neural feedback; and (ii) it only allows inferences about the *initial* response of neural feedback to a kinematic deviation. For example, if a sensory perturbation is assumed to create an *illusion* of a kinematic deviation of given type, then the initial muscular response to the sensory perturbation reflects how neural feedback would respond to an actual kinematic deviation of the same type. In this study, we use a combination of both approaches to infer the strategies used for the neural control of human walking.

### Specific aims

The aim of this study is to investigate the kinematic and muscular responses of treadmill walking to continuous external mechanical and visual perturbations. We expect these responses to have four general properties. First, we expect to see zero-latency open-loop responses to mechanical perturbations, which indicate that the perturbations were effective. Second, in alignment with literature [O'Connor and Kuo, 2009], we expect to see some type of active control strategy used for stabilizing walking. Third, similar to Logan et al. [2017], we expect that the responses of the nervous system to both perturbations will depend strongly on the phase at which the perturbation is applied. Lastly, we expect to see muscular responses at phases of the gait when the muscles are normally active. Further studying these responses will provide us with additional information on how the nervous system uses sensory information to stabilize walking.

*Thesis Organization*

In the next chapter, a review of literature will discuss general knowledge about stabilizing locomotion and how this knowledge has been incorporated into neuromechanical models of locomotion. Chapter 3 will describe the methods used in this experiment, including equipment, experimental design, data collection and data analysis. In chapter 4 we will present the results. Finally, in chapter 5 we will discuss what our results suggest about neural feedback control of human locomotion and directions for future studies.

## Chapter 2 : Literature Review

In this study, we seek to address how the nervous system stimulates the muscular system to provide stability and regulate walking. To this end, in this section we will first discuss some general knowledge regarding the neural control of locomotion obtained from physiological studies. In the next step, we will review current models of the neural control of human locomotion with the focus on their control strategies for stabilizing walking. Finally, we will discuss these strategies in a study done by Logan et al. [2017] that has quantified the responses of walking to small perturbations.

### *What is known about neural control of locomotion from physiological studies?*

During rhythmic gait, the nervous system stimulates muscles at specific phases of the gait cycle. For instance, the tibialis anterior is activated during swing to ensure foot clearance and during late swing and the initial stance phase, presumably to prevent the foot from slapping the floor [Boakes and Rab, 2006]. Another example is rectus femoris. This muscle is active during early stance and during the stance-to-swing transition, and it has been suggested that its activity during the stance-to-swing transition contributes to cadence regulation [Boakes and Rab, 2006]. The continuous modulation of these muscle activation patterns might also serve to control speed and stabilize gait. For instance, Kiemel et al. [2016] suggested that tibialis anterior activity is modulated immediately after heel strike to help control walking speed. In this chapter, we will review some of the strategies that the nervous system uses to regulate walking, but first let us review the mechanism through which the neural control operates.

Neurophysiological studies of animal locomotion have revealed the existence of a rhythm-generating network in the spinal cord, called a central pattern generator (CPG), which functions together with supraspinal areas of the central nervous system (CNS) to generate the basic locomotor rhythm [Dietz, 2003]. Sensory feedback modifies this rhythm to produce functional locomotion. Nonetheless, in principle CPG can produce basic rhythmic activity, even in the absence of sensory feedback. Indirect evidence suggests that the basic pattern of human locomotion may also be generated by a CPG that provides rhythmic activity to the leg extensor and flexor muscles [Hultborn and Nielsen, 2007]. As is the case for animal locomotion, sensory information is essential for human locomotor control. Stability in locomotion depends on the integration of

visual, somatosensory and vestibular inputs into central neuronal networks. Figure 2-1, depicts a schematic diagram of the components of locomotor control.

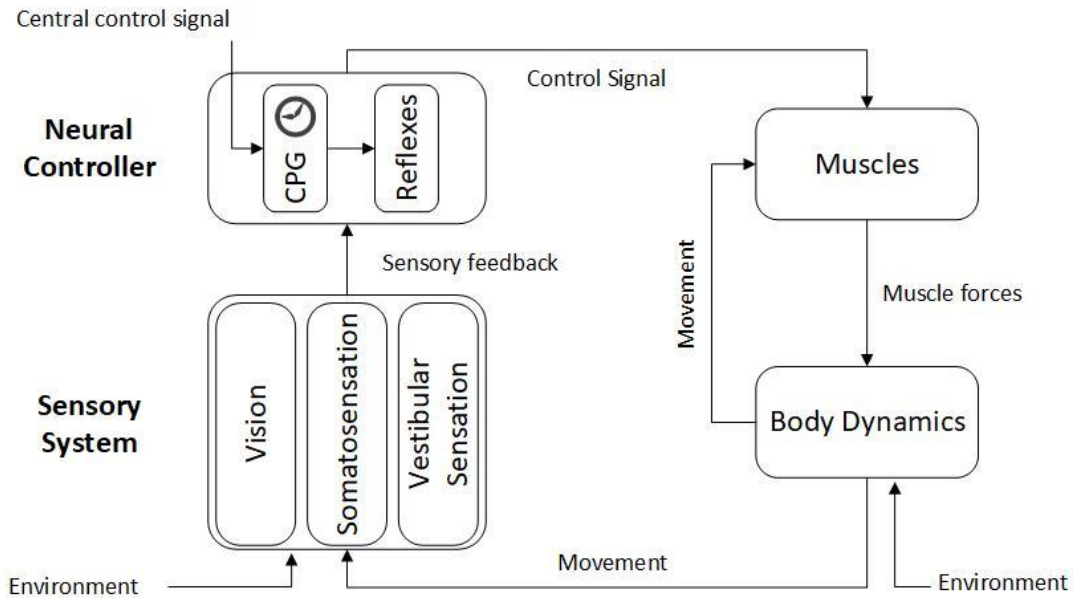


Figure 2-1) Schematic diagram of the components of locomotion control (inspired by Pearson et al. [2006] and Kiemel et al. [2008]).

Experimental studies on human locomotor responses to external perturbations have demonstrated that these sensory inputs are used by two classes of control mechanisms: anticipatory control and reactive control [Mori et al., 2004]. In the next section, we review some of this evidence.

#### Evidence of Anticipatory Control of Locomotion

Anticipatory control, as its name implies, relies on prediction of future sensory and motor events. At the heart of this control strategy is a clock that sets the neural command. Patla [2003], who uses the term “proactive” instead of “anticipatory”, categorizes this general class into two main strategies: 1) planning future movements based on expected perturbations that happen during walking (e.g., the ground reaction impact at heel strike); and 2) adjusting ongoing movements in face of unexpected external perturbations based on sensory input (e.g., obstacle avoidance). The first strategy is dictated by the phase of the gait cycle. For instance, Winter [1995] found that the trunk muscles activate prior to heel strike in order to counteract the unbalancing hip deceleration that occur at heel strike and keep the trunk erect. Similarly, Tibialis



Anterior (TA) activates prior to heel strike in anticipation of ground reaction forces. The second strategy is dependent on sensory input, usually from vision. There are two different ways of using sensory input in anticipatory control. The system can reset the phase of the gait cycle and use the same gait pattern, or it can modify the gait pattern. Phase resetting has been observed in animal studies (e.g. [Conway et al., 1987]); in addition, modeling studies (e.g. Aoi et al. [2010]) have suggested that this mechanism may contribute to the generation of adaptive human locomotion. The gait pattern modification strategy has been reported to occur in response to unexpected perturbations. Specific changes in the pattern of ground reaction forces (GRFs) and electromyograms (EMGs) has been reported in walking during obstacle avoidance [McFadyen and Winter, 1991; Patla et al., 1991]. For instance, it has been observed that nervous system adopts an active knee flexion strategy during obstacle avoidance, which is not observed in walking on level terrain.

### Evidence of Reactive Control of Locomotion

Unlike anticipatory control strategies, reactive control does not need an inner clock. Reactive control used by the nervous system relies on sensory information to counteract unexpected internal and external perturbations. Physiological studies have indicated that sensory feedback has two major roles in the regulation of locomotion [Pearson et al., 2006]. The first role is setting the timing of transitions from one phase of the gait cycle to the next. In one study, Pang and Yang [2000] showed that the position of the hip joint contributes greatly to the stance-to-swing transition. Another role of reactive control strategies is reinforcing ongoing muscle activity. For instance, several studies [Grey et al., 2004; Yang et al., 1991] have established the important contribution of proprioceptive feedback in enhancement of the ankle extensor muscle activation, particularly during the late part of the stance phase in walking.

In the next section, we review how models of human locomotion has incorporated these strategies in their control mechanisms.

### *Stabilizing Mechanisms in Neuromechanical Models*

Simulation studies have investigated the role of the nervous system in stabilizing locomotion. These studies can provide us with additional insights regarding the neural control of movement that would be difficult or even impossible to obtain from physiological studies alone [Pearson et al., 2006]. Models of human locomotion seek to answer two main questions: 1) why does neural control produce the periodic mean kinematic and EMG waveforms observed during gait; and 2) how does the controller correct deviations away from these mean waveforms? In order to answer the first

question, predictive optimal control methods are usually used that minimize a specific cost function, such as metabolic cost [Anderson and Pandy, 2001; Bhargava et al., 2004]. On the other hand, in order to answer the second question, the model should have a feedback component that corrects for the perturbations in the system. In this study, we are interested in the answer to the second question.

Here, we will give a brief review of models of walking with a neural component that is responsible for stabilizing walking. Historically, there are two main categories of models of human locomotion based on their neural components: 1) reactive control models and 2) anticipatory control models. Models in both categories include a number of muscles described with standard Hill-type models. The muscles forces are used as input to a mechanical model of the body and its environment, producing kinematics and ground reaction forces that result in locomotion. The difference between these models is in how the stimulation to muscles is generated and how it controls locomotion.

### Reactive Control Models

The reactive control models of human locomotion focus on the role of reflexes in producing rhythmic gait and stabilizing the movement. These models do not use an inner clock; instead they are hybrid systems that use different sets of control rules in different parts of the gait cycle (stance and swing, for instance). In these models, the influences of the sensory signals are captured by modifying the timing and magnitude of muscle activity in a manner that mimics physiological data.

*Reflex-based Model for Walking [Geyer and Herr, 2010]*

Geyer and Herr [2010] developed a sagittal-plane model of human locomotion that is controlled by muscle reflexes. This model is inspired by several physiological studies on the reactive control strategy of locomotion. The model is based on the core finding that a spinal reflex of extensor muscles during early stance reinforces activation in these muscles [Grey et al., 2007]. In addition, an earlier model of human locomotion [Geyer et al., 2003] also established that such positive force feedback of leg extensor muscles generate compliant leg behavior in stance and can produce periodic bouncing. From this paradigm, Geyer and Herr [2010] developed a model of human walking in which the extensor muscles with positive force feedback were responsible for providing the compliant behavior, and flexor muscles with positive length and force feedback were responsible for preventing joint overextension. The trunk control strategy in this model was inspired by O'Connor and Kuo [2009], who suggested that balancing the trunk might be achieved through trunk proprioceptive feedback. This model stabilizes the trunk movement by activating the hip muscles proportional to the velocity of the trunk

and to its forward lean (a proportional-derivative (PD) controller). In addition, a swing control strategy enables the model to enter cyclic locomotion. The extensor muscles activation during swing depended on the other leg's GRF in an inhibitory fashion, which reflexes on the physiological studies that relate the stance to swing transition to leg-unloading [Dietz and Harkema, 2004]. Using these feedback control strategies for generating the muscle activation, Geyer and Herr [2010] were able to reproduce much of the known muscle-activation and kinematic patterns of human gait. However, this model lacks an anticipatory control strategy; as a result, the activations of muscles that are presumably driven by anticipatory control strategies differ from activations during human gait. For instance, the activity of the tibialis anterior muscle prior to heel strike is lower than that of experimental data. In addition, the model lacked an explicit mechanism to control locomotor speed. In a later version of this model, Song and Geyer [2012] added a preliminary speed control strategy by tuning feedback gains. In general, this reactive model of locomotion mimics basic human kinematic and is also able to tolerate ground disturbances and adapt to slopes without the need for parameter interventions.

### *Equilibrium Point Model with feedback for Walking [Günther and Ruder, 2003]*

Günther and Ruder [2003] developed a sagittal-plane model of human gait that is controlled through the changes in the *referent* body configuration. This model is based on the equilibrium point hypothesis (EPH) in which Feldman and Levin [1995] suggested that the central nervous system (CNS) uses nominal muscle length,  $\lambda$  (the threshold length beyond which the muscle will produce force) as a physiological variable to control movement. In this model, the muscle stimulation is a function of both the nominal muscle length and the actual muscle length. The feedforward part of the neural control consists of just two target configurations ("lift knee" and "set foot") each of which is composed of a set of nominal lengths for each muscle. The neural controller switches between these two target configurations each step cycle, while assigning the opposite configuration to the contralateral leg. This model uses a reactive control strategy, since the timing of the movement is not predetermined by an inner clock, but it is triggered by feedback signals of the mechanical state of the musculoskeletal system (ankle AP position and the GRF). In addition, the model maintains the balance of the upper body through proprioceptive feedback strategy. Like the Geyer and Herr [2010] model, this model balances the trunk using a simple control strategy that does not require multisensory information. The upper body is stabilized by continuously modifying the nominal length of hip muscles of the stance leg based on the sensory feedback of trunk angle and horizontal velocity. Using these neural strategies, the model's kinematic and muscular stimulations were found to be in

agreement with experimental patterns. Günther and Ruder [2003] also found that this model tolerates small slope changes without the need for parameter adjustments.

### Models with Anticipatory Control

Models of locomotion that use anticipatory control strategies have a CPG whose output represents motoneuron pool activity that provides stimulation to muscles. This muscle stimulation is then transformed via muscle models into forces. In these models, sensory inputs have two main effects. First, sensory inputs can reset the phase of the gait cycle by, for example, triggering a transition from one state to another. Phase resetting then affects muscle stimulation. Second, sensory inputs directly affect muscle stimulation via reflexes. As a result, these models have both an anticipatory phase-dependent component and a sensory-feedback component [Pearson et al., 2006]. The anticipatory phase-dependent component produces the basic output pattern of muscle stimulation even without sensory feedback. Sensory feedback modifies this basic pattern directly via reflexes and indirectly via phase resetting. The combination of these two components produces motor output similar to that observed in human gait.

#### *CPG Model of Human Locomotion [Taga, 1995]*

Taga [1995] developed a model of human locomotion that relies on anticipatory control strategies. Inspired by the neural circuits in the nervous system that have been associated with rhythmic movement, the neural controller in this model consists of a rhythm generator that excites seven neural oscillator pairs (one for the trunk and two for each pair of hip, knee, and ankle joints), each of which control the muscles around a single joint via inhibitory connections. The active periods of muscles are determined by the system's "global" state. The locomotion model has a sequence of six global states that depend on the phase of the gait cycle and are computed by the central neural system. The neural model also has a mechanical impedance controller that regulates musculoskeletal properties (such as stiffness and viscosity) as a function of body state. The sensory feedback in this model provides input to the three components of neural controller. The global sensory information is provided by the central neural system that computes the state of the body using the angle of an inverted pendulum from COP to COM, and the "local" sensory information is provided by the adjacent segments. Using this model, Taga [1995] was able to produce stable locomotion that was quantitatively similar to human walking.

#### *Phase Resetting Model of Human Locomotion [Aoi et al., 2010]*

Aoi et al. [2010] developed a physiological model of the neural system for locomotion that emphasized the role of phase resetting in stabilizing the system. The

neural controller in this model consists of a CPG model based on a two-layered hierarchical network model of the rhythm generator (RG) and pattern formation (PF) networks. The RG network produces rhythm information using phase oscillators and regulates it by phase resetting. The PF network shapes the rhythm into spatiotemporal patterns of activation of motoneurons and creates feedforward command signals composed of combinations of five rectangular pulses. In addition, this model has a postural control strategy that uses feedback to regulate the trunk angle. Sensory feedback information is also used to reset the phase of the gait cycle based on foot-contact timing. Simulation results showed that this model establishes adaptive walking against perturbing forces and variations in the environment.

A Model with both Anticipatory and Reactive Control

*CPG Dependent Reflex-based Locomotion Model [Dzeladini et al., 2014]*

Recently, Dzeladini et al. [2014] developed a neuromuscular model of locomotion that incorporated the anticipatory control strategy of CPG-based models (inspired by [Kuo, 2002]) into the reflex-based locomotion model of Geyer and Herr [2010]. Dzeladini et al. [2014] modified the Geyer and Herr [2010] reflex-based model, eliminating the direct mapping from sensory input to muscles activation by incorporating intermediate stages such as interneurons and motoneurons. The CPG in this model is considered to be a feedback predictor (anticipatory control) and contributes to speed control, which was difficult to achieve in the original reflex-based model.

The models reviewed in this section have been used to examine the feasibility of various control hypotheses by comparing their mean periodic behavior with experimental data. However, these models have not been tested in how they would response to small continuous perturbations, and very little experimental data on this subject exists.

*What is known about the control based on experimental data?*

Few studies have used small mechanical perturbations to investigate the mechanisms used to provide stability in human walking [Logan et al., 2017; Moore et al., 2015], large transient perturbations being more commonly used (e.g., [Grey et al., 2004; Grey et al., 2007; Yang et al., 1991]). Here we focus on Logan et al. [2017], since this study used experimental and analysis methods similar to those of the current study. [Logan et al., 2017]

Logan et al. [2017] studied the responses of human locomotion to continuous mechanical and sensory perturbations. They perturbed walking mechanically using a spring attached to the upper trunk at one end and a linear motor at the other end. They also perturbed walking using virtual visual-scene motion. Computing the muscular and kinematic response of the system to the perturbation signals, Logan et al. [2017] detected indications of active neural control; they observed a muscular responses to both classes of perturbations as well as a phase shift effect. They also found that the muscular responses to the perturbations depended on the phase of the gait cycle, and the muscles were found to be modulated at the phases of the gait when the muscles are normally active. In addition, they found indications of reactive control strategies. For instance, in response to the mechanical perturbations, Logan et al. [2017] found a counteracting muscular response during late swing phase of either foot, a reactive strategy which is similar to Winter [1995] “balancing moment.”

This study follows up on the work done by Logan et al. [2017]. Here we apply lower leg mechanical perturbation that aim to help us better understand the stabilizing mechanisms used in walking that concern foot placement.

## Chapter 3 : Methods

### Subjects

Twenty healthy individuals: nine men with age  $20.2 \pm 1.3$  (mean  $\pm$  SD) years, height  $1.81 \pm 0.06$  m, weight  $78.9 \pm 8.1$  kg and eleven women with age  $21.9 \pm 1.7$  years, height  $1.60 \pm 0.07$  m, weight  $62.0 \pm 13.2$  kg were recruited through undergraduate courses to participate in this study. The protocol was approved by the University of Maryland's Institutional Review Board, and all participants completed an informed consent process before continuing with the study. They also completed a health history questionnaire and none of them were found to have a history of musculoskeletal disorders or neurological deficits or used prescription drugs that affect balance.

### Procedure

#### Protocol

The subjects walked on a treadmill (Cybex Trotter 900T, Cybex International, Inc., USA) facing a single visual display (width: 3.05m, height: 2.44m; Fakespace). Each subject walked at the speed of 5.0 km/h (1.4 m/s) for 12 trials of length 250 s. For all trials other than the first and last one, the perturbation apparatus described below was attached to their ankles as they walked.

The visual display was rear-projected to the screen at a frame rate of 60Hz by a JVC projector (model DLA-M15U; Victor Company of Japan). The display, when the visual scene was stationary, consisted of 500 white small triangles ( $3.4 \times 3.4 \times 3.0$  cm) with random positions and orientations on a black background. Triangles were excluded from a black 30-cm-radius circular region whose center was immediately in front of the participant's eyes. The subjects were instructed to look straight ahead at this region, in order to reduce the aliasing effects in the foveal region. The sensory perturbation consisted of virtual sagittal-plane rotation of the visual scene about a fixed medial-lateral axis roughly through the mean positions of the subject's ankles. CaveLib software (Fakespace) was used to generate the virtual movement based on a fixed perspective point approximately at the position of the subject's eyes. The virtual rotation angle was specified by the sensory perturbation signal described below.

The mechanical perturbation was applied to the subject's lower extremities through a spring and pulley system. Subjects wore ankle supports that were connected to each other with a cord sliding on a light pulley (Figure 3-1). A weak spring (spring constant: 0.00875 N/mm) was attached at one end to the pulley and at the other end to a linear-motor (LX80L; ParkerHannifin Corporation) placed directly behind the subject. This mechanism exerted a weak backward pull on both legs, whose primary kinematic effect was a small backward deviation of the swing leg at any point in time. The actual displacement of the motor was used as the mechanical perturbation signal. The force applied to the legs in this system is a function of both the displacement of the motor and the leg; therefore, force could not have been chosen as the input variable. In an alternative experimental design, rather than specifying motor position and using a weak spring, one could directly specify small forces applied to the legs. Results in this

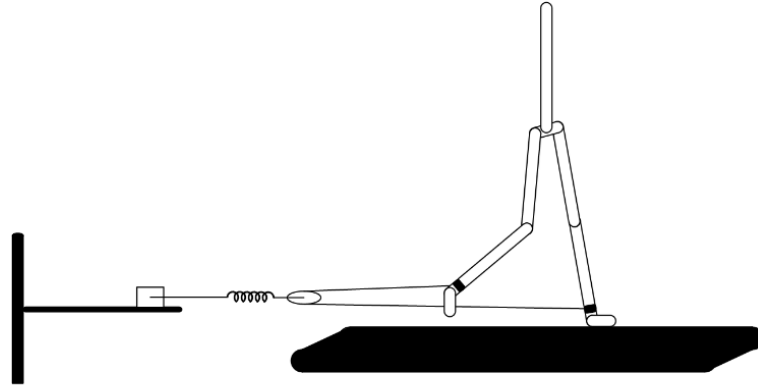


Figure 3-1) Schematic figure of the mechanical perturbation.

alternative force-control experiment would be expected to be similar to our results, except that responses would be scaled by one over the spring constant (refer to [Logan et al., 2017] for more information).

Filtered white noise signals were used for the perturbation signals. To generate each perturbation signal, we started with a 230-s white noise signal with power spectral density of  $P$ . Different seeds were used for the sensory and mechanical perturbation signals to ensure statistical independence. Therefore, we could use simultaneous perturbations and still be able to separately identify the effect of each perturbation on the output signals. The signal was then passed through a first-order filter with cutoff frequency of  $f_{c1}$  and an  $m$ -order Butterworth filter with a cutoff frequency of  $f_{c2}$ . In both cases, we needed the perturbation signals to be small enough to not cause a drastic change in the control strategy, while big enough to produce a detectable response. For the visual perturbation, we used the following parameters:  $m = 2$ ,  $P = 150 \text{ deg}^2/\text{Hz}$ ,  $f_{c1} = 0.02 \text{ Hz}$ , and  $f_{c2} = 5 \text{ Hz}$ . Visual perturbations with these parameters produced



detectable kinematic and EMG responses in a previous study [Logan et al., 2017]. For the mechanical perturbation, the first-order filter was not used. Because of the mechanical limits of the motor, there is a trade-off between increasing  $P$  and  $f_{c2}$ . Based on a pilot study, we chose parameters  $m = 8$ ,  $P = 3.1 \text{ cm}^2/\text{Hz}$ , and  $f_{c2} = 2.6 \text{ Hz}$ . The initial and final 5 s of the 230-s signal were multiplied by increasing and decreasing ramps, respectively, to ensure that the value of the signal started and ended with a value of 0. Finally, 10-s windows with a constant value of 0 were added to the beginning and the end of the signal, resulting in a 250-s signal for the given trial. Only the middle 220 s of each trial were used for response analysis.

### Data collection

#### *Kinematic Data*

The kinematic data were recorded using a ten camera VICON-MX motion analysis system (VICON, Inc, Oxford, UK) at the rate of the 120 Hz. Reflective markers (diameter, 1.4 cm) were placed on the right and left sides of the body at external landmarks: base of the 5th metatarsal, posterior calcaneus (heel), lateral malleolus (ankle), lateral femoral condyle (knee), greater trochanter (hip), anterior superior iliac spine (ASIS), posterior superior iliac spine (PSIS), iliac crest, superior acromion process (shoulder), mastoid process (head) and frontal eminence (head). Additionally, markers were placed at the mediolateral center of the back of the head and the midline of the spine at the level of C7, T10 and L1 vertebrae. All markers were attached at the skin of these bony prominences except those that were placed on the shoe (at the 5th metatarsal and heel).

#### *EMG Data*

Muscular activity of the right leg and trunk were measured using surface electromyographic (sEMG) recordings. The sEMG data were recorded at 2160 Hz using the wireless TRIGNO system (DELSYS, USA) which has built-in bandwidth of 20–450 Hz and gain of 909 V/V. The sEMG electrodes were positioned on fourteen muscles according to previous recommendations [Criswell, 2010], in order to minimize cross-talk. The sEMG were collected from: tibialis anterior (TA), gastrocnemius lateralis (LG), gastrocnemius medialis (MG), soleus (Sol), vastus medialis (Vmed), vastus lateralis (Vlat), rectus femoris (RF), tensor fascia latae (TFL), biceps femoris (BF, long head), semitendinosus (ST), gluteus Maximus (GM), gluteus medius (Gmed), rectus abdominus (RA), and lumbar erector spinae (ESL, recorded at L1-L2). Recording sites were shaved, lightly abraded, and cleaned with isopropyl alcohol prior to electrode application.

### Data Analysis

The sensory perturbation signal was the angular velocity of the specified visual-scene rotation in units of deg/s. The mechanical perturbation signal was the measured anterior-posterior position of the motor in units of cm. In order to measure the kinematic and muscular response to these external perturbations, first the data had to be processed and then analyzed.

#### Signal Processing

##### *Kinematic Data*

The kinematic data were analyzed in the sagittal plane. The segment angles were computed relative to vertical, with positive indicating that the upper end of the segment moved forward relative to the lower end. The joint angles were computed by subtracting the lower segment angle from the upper one. Finally, the markers' displacement and velocity in the AP direction were measured.

##### *EMG Data*

Using Matlab, the EMG signals were high-pass filtered using a zero-lag forward-backward cascade of a 4th-order Butterworth filter with a 20-Hz cutoff frequency and then full-wave rectified.

#### System Identification

To describe how a limit-cycle system responds to any small perturbation, it is sufficient to describe how it responds to a small brief perturbation (an impulse) at any phase of the gait cycle, that is, its phase-dependent impulse response function ( $\phi$ IRF). A  $\phi$ IRF describes the effect of an input  $u(t)$ , here a sensory or mechanical perturbation signal, on an output  $y(t)$ , here a kinematic or EMG signal. Computing the  $\phi$ IRF for a limit-cycle system based on responses to small continuous perturbations is complicated by the fact that the perturbations can reset the phase of the gait cycle [Kiemel et al., 2016; Logan et al., 2017]. First, the phase of the gait cycle must be estimated and response variables expressed as functions of the phase. Then, harmonic transfer functions (HTFs) should be computed to characterize responses in the frequency domain. Finally, the HTFs must be converted to a  $\phi$ IRF in the time domain. Here, the details and the steps of this procedure will be explained.

1- *Phase Estimation and Replacement*

Local minima of heel vertical position was used to indicate the heel-strikes times  $t_k$  ( $k = 1, \dots, K$ ) for the reference leg. The average stride time ( $\bar{T}$ ) was calculated and used to compute the gait frequency as  $f_0 = 1/\bar{T}$ . The approximate phase of the gait cycle ( $\theta_d(t)$ ) was defined as a linear function of time between each heel-strike:

$$\theta_d(t) = k + f_0(t - t_k) \quad t_k \leq t < t_{k+1}. \quad (3-1)$$

The  $\theta_d(t)$  is a causal discontinuous signal. In order to compute a continuously-differentiable estimate of the phase,  $\theta(t)$ , a second-order low-pass filter with rate constant of  $d = 2$  was applied to  $\theta_d(t)$ :

$$\ddot{\theta}(t) + 2d(\dot{\theta}(t) - f_0) + d^2\theta(t) = d^2\theta_d(t). \quad (3-2)$$

The estimated phase  $\theta(t)$  is a function that maps time to phase. In order to express the data as a function of phase, a new independent variable should replace time. We defined approximate phase  $\vartheta$  as the independent variable, and let it replace time  $t = p(\vartheta)$ , where  $p(\vartheta)$  is the inverse function of  $\theta(t)$ . The input and output variables as functions of  $\vartheta$  became  $\tilde{u}(\vartheta) = u(p(\vartheta))$  and  $\tilde{y}(\vartheta) = y(p(\vartheta))$ , respectively. Also, we defined the following derivative:  $\tilde{d}(\vartheta) = \dot{\theta}(p(\vartheta))/f_0$ . (All the steps applied to  $\tilde{y}(\vartheta)$  were also applied to  $\tilde{d}(\vartheta)$  from this point to step 5.)

2- *Identifying Perturbation Reponses*

In order to proceed to the perturbation analysis, first the perturbed response should be distinguished from the unperturbed response. Therefore, we subtracted the mean pattern from the signals:  $\tilde{y}^{(1)}(\vartheta) = \tilde{y}(\vartheta) - y_0(\vartheta)$ , where  $y_0(\vartheta)$  is the mean of  $\tilde{y}(\vartheta)$ , and  $\tilde{y}^{(1)}(\vartheta)$  is the deviation away from the mean.

*Spectral Analysis*

The next step is to apply spectral analysis to the input and output signals. For two signals  $\tilde{u}(\vartheta)$  and  $\tilde{y}^{(1)}(\vartheta)$  their power spectral densities (PSDs),  $p_{\tilde{u}\tilde{u}}(f_1)$  and  $p_{\tilde{y}\tilde{y}}(f_2)$ , and the double-frequency cross spectral density (CSD),  $p_{\tilde{u}\tilde{y}}(f_1, f_2)$ , were computed [Bendat and Piersol, 2011], where  $f_1$  is the input frequency, and  $f_2$  is the output frequency. The PSD and CSD was calculated using the Welch's method. The signals were divided into  $n_w$  windows of length  $n_c = 20$  with 50% overlap. Hanning windows,  $w(\vartheta) = (1 - \cos(2\pi\vartheta/n_c))/2$ , were multiplied with these windows of data:  $\tilde{u}_l(\vartheta) = w(\vartheta)\tilde{u}(\vartheta)$ .  $\tilde{U}_l(f_1)$  and  $\tilde{Y}_l(f_1)$ , the Fourier transforms of the windowed signals  $\tilde{u}_l(\vartheta)$  and  $\tilde{y}_l(\vartheta)$  were computed. (Throughout this section, lower case letters denote time

domain quantities and the corresponding capital letters indicate the respective Fourier transformed functions.) Finally, the PSD and CSD were estimated using:

$$p_{\tilde{u}\tilde{u}}(f) = \frac{1}{n_w \bar{w}} \sum_{l=0}^{n_w-1} |\tilde{U}_l|^2 \quad (3-3)$$

$$p_{\tilde{u}\tilde{y}}(f_1, f_2) = \frac{1}{n_w \bar{w}} \sum_{l=0}^{n_w-1} \tilde{U}_l(f_1) \tilde{Y}_l^*(f_2) \quad (3-4)$$

where  $\bar{w}$  is the mean square of  $w(\vartheta)$ , and the asterisk '\*' denotes complex conjugation.

In the next step, we explain how the closed-loop input-output mapping from  $\tilde{u}(\vartheta)$  to  $\tilde{y}(\vartheta)$ :  $H_{\tilde{u}\tilde{y}}(f)$  were calculated in the frequency domain using harmonic transfer functions (HTFs).

#### *Computing HTFs*

A HTF is an extension of the frequency response function (FRF) from LTI to LTP systems [Möllerstedt and Bernhardsson, 2000]. In an LTP system, input at frequency  $f$  produces output at frequencies  $f + kf_0$ , where  $k$  is an integer. Therefore, the input-output mapping of an LTP system is described by HTFs:  $\tilde{Y}(f) = \sum_{k=-\infty}^{\infty} H_{\tilde{u}\tilde{y},k}(f - kf_0) \tilde{U}(f - kf_0)$ , where  $\tilde{U}(f)$  and  $\tilde{Y}(f)$  are Fourier transforms of  $\tilde{u}(\vartheta)$  and  $\tilde{y}(\vartheta)$ . Walking with phase,  $\vartheta$ , as the independent variable is an approximately LTP system. As the result, we can use HTFs for computing the response of the system. In order to do that, first the modes of the HTF should be computed. We used PSDs and CSDs to calculate the  $k^{\text{th}}$  mode of  $H_{\tilde{u}\tilde{y}}(f)$  for each trial:

$$H_{\tilde{u}\tilde{y},k}(f) = \frac{p_{\tilde{u}\tilde{y}}(f_1, f_1 + kf_0)}{p_{\tilde{u}\tilde{u}}(f_1)} \quad (3-5)$$

#### *Using HTFs to Compute Phase Dependent Impulse Response Functions ( $\phi$ IRF)*

$\phi$ IRFs describe the reaction of the system as a function of phase:  $\tilde{y}^{(1)}(\vartheta_r) = \int_{-\infty}^{\vartheta_r} h_{\tilde{u}\tilde{y}}(\vartheta_r, \vartheta_s) \tilde{u}(\vartheta_s) d\vartheta_s$ . (Keep in mind that the  $\phi$ IRF  $h_{\tilde{u}\tilde{y}}$  is a function of both response phase  $\vartheta_r$  and the stimulus phase  $\vartheta_s$ .) In order to calculate the  $\phi$ IRFs, the HTFs should be transformed to the phase domain, then  $\phi$ IRFs should be adjusted to change back from phase to time as the independent variable. We took the inverse Fourier transform of each mode of the HTFs (both transient ( $H_{\tilde{u}\tilde{y}}(f)$ ) and phase-derivative

( $H_{\tilde{u}\tilde{a}}(f)$ ) and calculated the transient ( $h_{\tilde{u}\tilde{y}}(\vartheta_r, \vartheta_s)$ ) and phase-derivative ( $h_{\tilde{u}\tilde{a}}(\vartheta_r, \vartheta_s)$ )  $\phi$ IRFs. We then computed the phase  $\phi$ IRF by integrating the phase-derivative  $\phi$ IRF:  $h_{u\theta}(\vartheta_r, \vartheta_s) = \int_{\vartheta_s}^{\vartheta_r} h_{\tilde{u}\tilde{a}}(\vartheta, \vartheta_s) d\vartheta$ . Finally combining the  $\phi$ IRFs  $h_{\tilde{u}\tilde{y}}$  and  $h_{u\theta}$ , we obtained the  $\phi$ IRF from  $u(t)$  to  $y(t)$  in the time domain:

$$h_{uy}(t_r, t_s) = f_0 h_{\tilde{u}\tilde{y}}(t_r, t_s) + y'_0(t_r) h_{u\theta}(t_r, t_s). \quad (3-6)$$

We used both sensory and mechanical perturbations as input of the system to study the kinematic and muscular responses. A positive impulse response indicates that the variable's response is in the same direction as the perturbation and a negative impulse response indicates that the variable's response is in the opposite direction as the perturbation. In the results section, we will use  $\phi$ IRF plots to describe the effects of the perturbations on human walking. Here, we give a brief overview on how to read these plots by analyzing some hypothetical responses.

#### *Hypothetical examples*

Figure 3-2 shows a hypothetical example in which the studied variable, hip anterior-posterior (AP) position, only responds to perturbations applied during the swing phase (perturbation phases -0.38 to 0). In this example, an impulse during the swing phase produces a positive transient response lasting from normalized response times 0 to 0.62 (Figure 3-2C first two columns). On the other hand, perturbations applied during the stance phase do not produce a response; as the result, the  $\phi$ IRF, which is the difference between the unperturbed and perturbed signal, is zero (Figure 3-2C last column). Figure 3-2D shows what this behavior would look like in a color contour plot. The  $\phi$ IRF plot has two independent variables: the phase of perturbation indicated on the horizontal axis and the normalized response time indicated on the vertical axis, which is time relative to heel strike expressed in units of mean cycle period. The black bars on the horizontal and vertical axes indicate values of 0 to 0.62 corresponding to stance for the reference leg. The  $\phi$ IRF plot has a single dependent variable that describes the sizes and directions of responses to perturbations. These  $\phi$ IRF values are represented using color from cold to hot: green for 0, red for positive, and blue for negative. The diagonal line in the contour plot corresponds to a response measured at the same time the perturbation is applied. By definition, the  $\phi$ IRF is 0 (green) below this line.

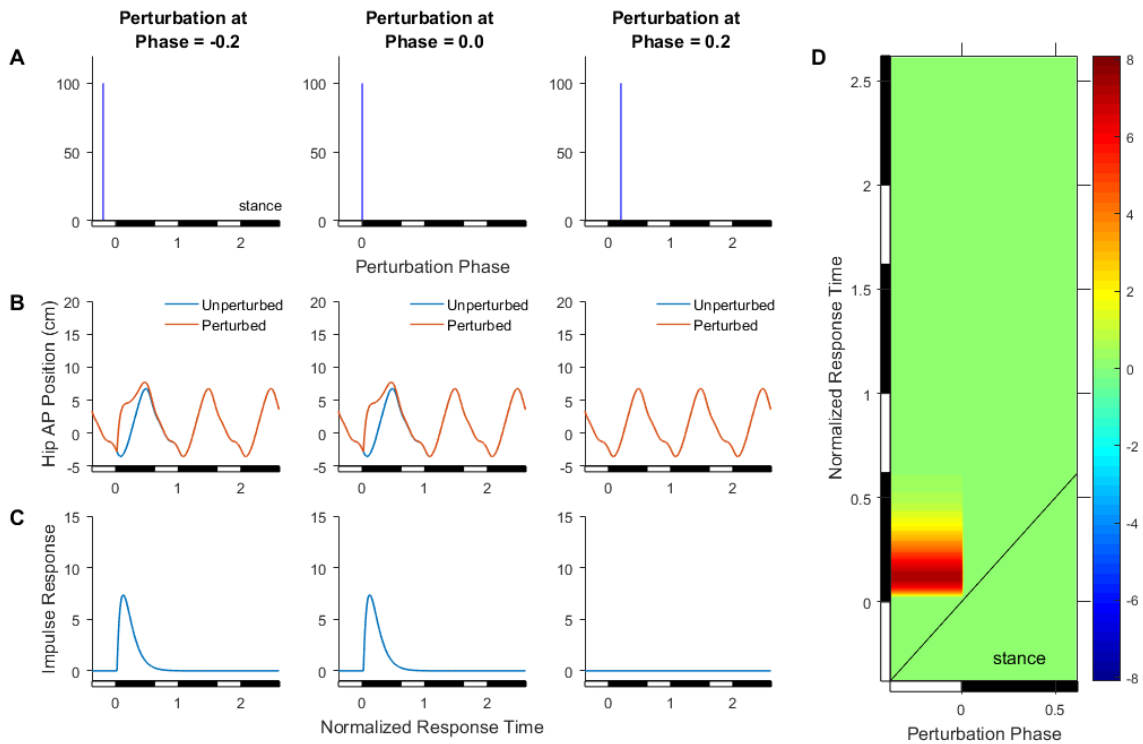


Figure 3-2) Hypothetical example #1 (swing response) A. The impulse applied to the system as a function of phase B. The mean waveform before and after the impulse (shown in blue and red respectively) as a function of normalized response time C. Impulse response as a function of normalized response time D. Hip AP position response (PD\_IRF).

In the next hypothetical example, the hip AP position undergoes a positive transient response after a constant delay from the onset of the impulse, for perturbations applied at all phases. The shape of the transient response in this example is similar to the previous one, but unlike the first example, here the response occurs at a fixed time delay after the perturbation (Figure 3-3C). This type of response is represented by a diagonal red (if positive) bar in the contour plot (Figure 3-3D). For a response that occurs immediately after the perturbation, this red bar will be shifted down to the diagonal line. Below, we refer to this type of response an “instantaneous” or “zero-latency”.

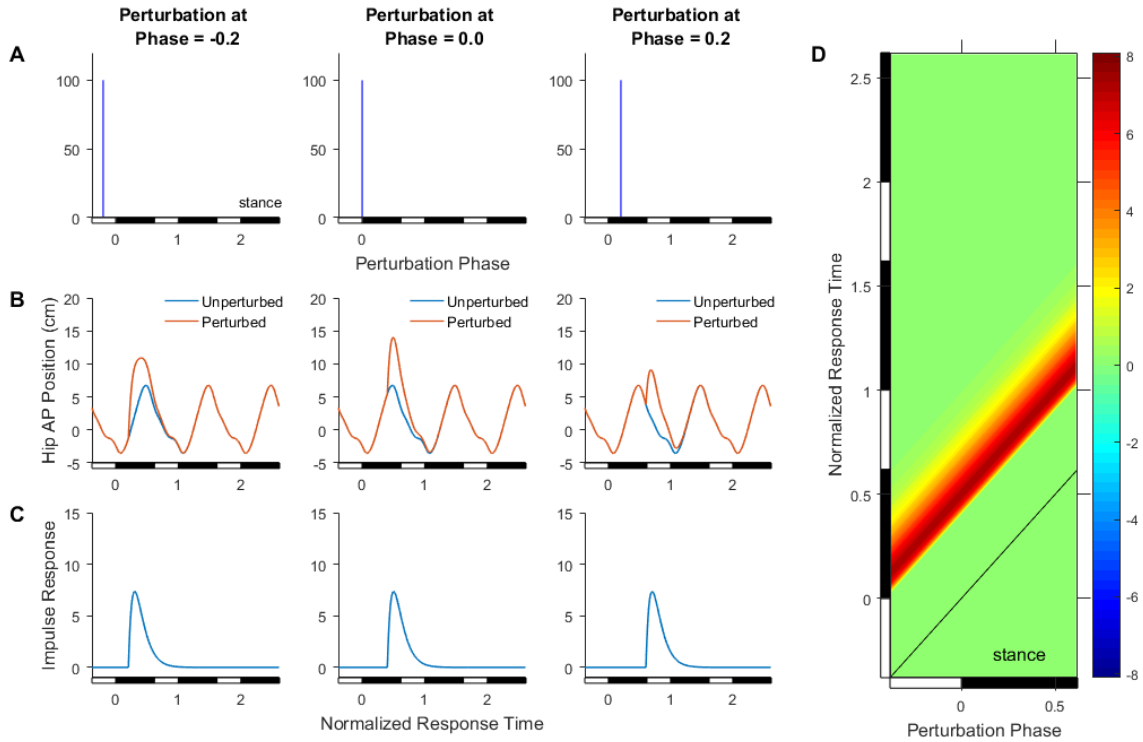


Figure 3-3) Hypothetical example #2 (constant delay) A. The impulse applied to the system as a function of phase B. The mean waveform before and after the impulse (shown in blue and red respectively) as a function of normalized response time C. Impulse response as a function of normalized response time D. Hip AP position response (PD\_IRF).

Finally, in the last hypothetical example, impulses applied at different perturbation phases cause a delay in the phase of the gait cycle that persist over the following cycles (Figure 3-4B). This phase shift results in repeating negative and positive responses (Figure 3-4C). The horizontal blue and red bars in the contour plot corresponds to this phase shift (Figure 3-4D).

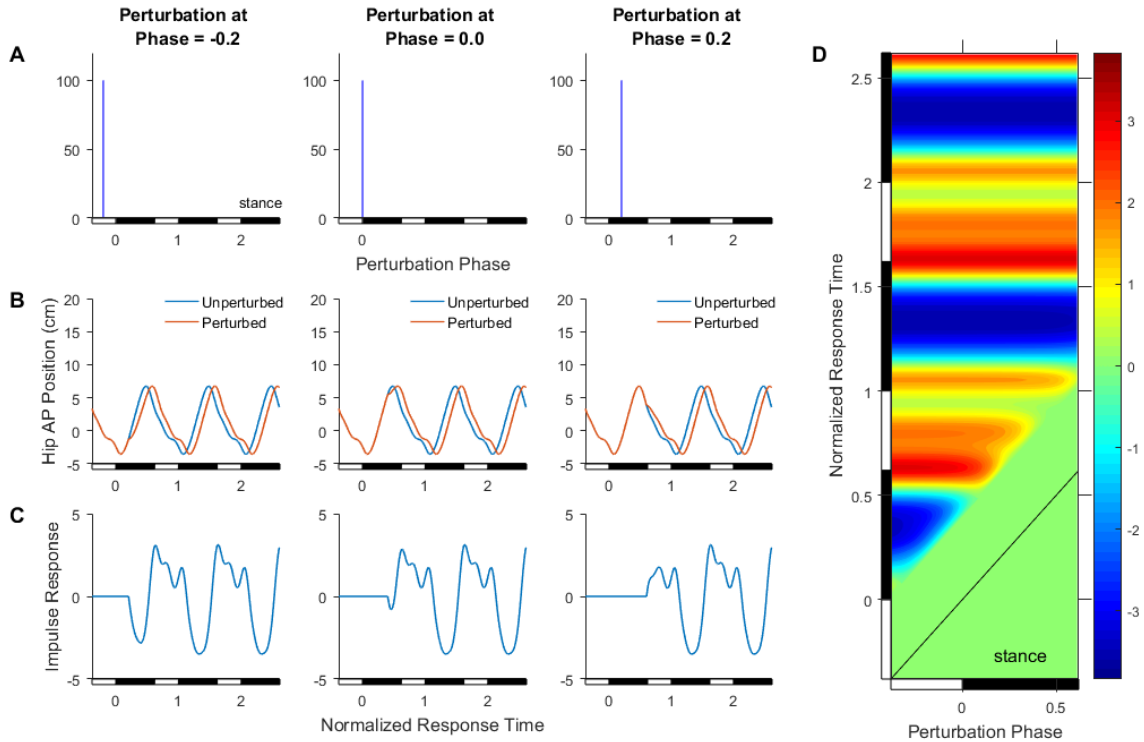


Figure 3-4) Hypothetical example #3 (phase shift) A. The impulse applied to the system as a function of phase B. The mean waveform before and after the impulse (shown in blue and red respectively) as a function of normalized response time C. Impulse response as a function of normalized response time D. Hip AP position response (PD\_IRF).

### Statistics

For each response variable, statistical tests were performed on the  $\phi$ IRF for all perturbation phases and for response times up to 3 cycles post stimulus onset. We used  $t$ -tests to determine whether  $\phi$ IRF values, averaged across multiple trials for a single subject then averaged across multiple subjects, are significantly different than zero. We also computed 95% confidence intervals.



## Chapter 4 : Results

The kinematic and muscular responses to mechanical and sensory perturbations were computed using the procedure described in the methods section. For each response variable, the phase-dependent impulse response function ( $\phi$ IRF) was calculated. In this chapter, we use  $\phi$ IRF plots to describe the effects of the perturbations on human walking

### Mechanical Perturbation

The mechanical perturbation was applied in 10 trials for most participants. (Due to technical difficulties, these perturbations were applied only in 9 trials for 4 of the 20 participants.) The mechanical perturbation signal was the motor displacement in mm, where forward movement of the motor was considered positive. In each case, we used  $\phi$ IRFs to describe the inferred effect of the motor briefly moving forward a small amount and then returning to its original position; the effect of backward movement of the motor was assumed to be equal in magnitude and opposite in direction.

#### Phase Response to Mechanical Perturbations

As mentioned in the methods section, the total response is composed of the response due to the effect of the perturbation on estimated phase and the transient response. As the result, the first variable we analyzed was the estimated phase. Figure 4-1 shows the response of the estimated phase to the mechanical perturbation. A negative  $\phi$ IRF is observed in response to perturbations applied in the swing and mid stance phase (which corresponds to the swing phase in the contralateral leg). This indicates that the mechanical perturbation at these periods produced a delay in the phase of the gait cycle that persisted thereafter.

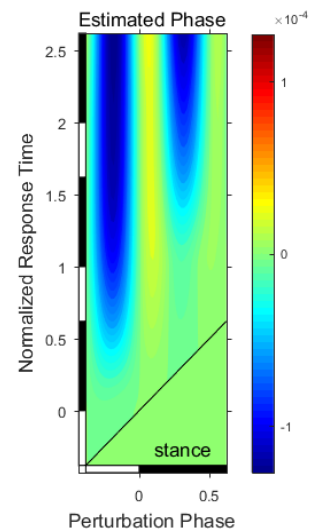


Figure 4-1) Estimated phase response to the mechanical perturbation

### Kinematic Responses to Mechanical Perturbations

Generally, we were able to detect significant responses for almost all kinematic variables to the mechanical perturbation. The responses were highly dependent on the phase of the perturbation, as well as the shape of the mean waveform. The kinematic variables showed an instantaneous response to the mechanical perturbations, ramping up or down after the onset of the perturbation. Here we illustrate these responses.

Let us start by discussing the response of the subjects' walking speed (based on the AP velocity of the midpoint between the two hip markers) to the motor displacement. As mentioned above, the mechanical perturbation caused a delay in the phase of the gait cycle. This effect can be better detected by breaking down the total IRF into its components: the transient IRF and the phase IRF. Figure 4-2 does this for the response of walking speed to the motor displacement. The phase delay causes the mean waveform (Figure 4-2D) to lag behind and produces an initial negative response in the IRF due to the phase (Figure 4-2B). This initial response is then followed by successive positive and negative responses that, as mentioned in the methods section, indicate a phase shift. Keep in mind that the response here is highly phase dependent; as the results the horizontal blocks are only present in response to perturbations applied during swing and mid-stance (which corresponds to the other leg swing phase).

The transient response, on the other hand, was initially positive following perturbations applied during the swing phase (Figure 4-2C.). This instantaneous response can be better observed by looking at slice of the  $\phi$ IRF plot. Figure 4-2E. takes a vertical slice through the contour plot (Figure 4-2C) at stimulus phase -0.24 and depicts the mean  $\phi$ IRF and 95% confidence interval to illustrate how this variable changes after the onset of the perturbation (indicated by the yellow arrow in Figure 4-2E). It is evident that walking speed responds without any delay to the perturbation. Combining these two IRFs, we can calculate the total  $\phi$ IRF which has an initial positive response to the perturbations during swing, followed by a phase shift. In other words, when the motor moves forward during swing, the subject increases his/her walking speed initially, and then this effect goes away and only the phase resetting effect remains. The variable of walking speed has left-right symmetry, meaning that it remains unchanged by switching left and right. For the  $\phi$ IRF for a response variable with left-right symmetry (e.g., Figure 4-2A), if the perturbation phase is delayed by half a cycle, then the response is the same except that it is also delayed by half a cycle. See Appendix A for more information about how symmetry is reflected in  $\phi$ IRFs.

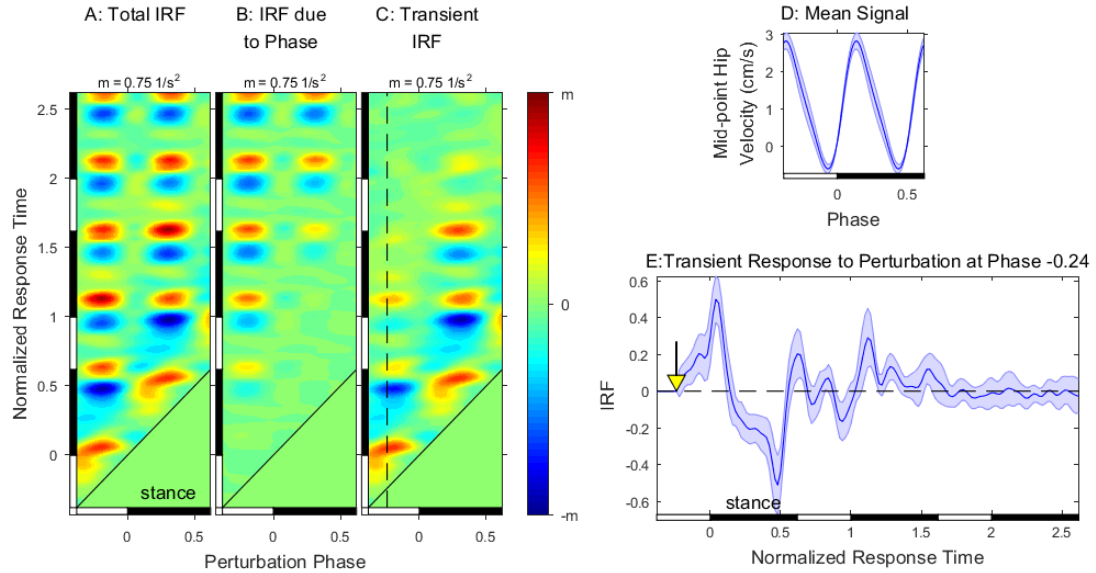


Figure 4-2) Mid-point hip velocity response to the mechanical perturbation, broken down to its components. A. Total  $\phi$ IRF B. IRF due to phase C. Transient IRF D. Mid-point hip velocity mean waveform and E. Transient response for the perturbations applied at phase -0.24. D. IRF values are in units of  $0.75 \text{ 1/s}^2$ . E. Shaded area is standard deviation.

From now on, we will only discuss the variable responses using the total  $\phi$ IRF response. Also, we will not show the color bar in each figure; the color coding represents  $\phi$ IRF values  $-m$  to  $m$ , where the value of  $m$  is given at the top of each  $\phi$ IRF contour plot.

Next, we present the responses of ipsilateral lower-body marker positions to the perturbation (Figure 4-3). The term “ipsilateral” denotes the side of the body used to define the phase of the gait cycle. It is evident that the  $\phi$ IRFs are highly phase-dependent. For AP positions, an initial positive response is observed for perturbations applied during swing (indicated by the black arrows in Figure 4-3A to E). Similar initial behaviors were seen for all AP responses; however, the magnitude of the  $\phi$ IRFs decrease for locations further up the perturbation point at the ankle. Along with these positive AP responses, the hip vertical position shows an initial negative response in this period (indicated by the black arrow in Figure 4-3F). In other words, when the backward pulling force on the ankles is decreased (or increased) during early swing phase, the ipsilateral lower body instantaneously moves forward (or backward) in the AP direction, while the ipsilateral hip marker lowers (or rises) in the vertical direction. Like all kinematic responses, the onset of responses here is instantaneous.

The horizontal red and blue blocks detected in heel, toe, ankle, knee AP position and hip vertical displacement responses, can be explain by the phase delay effect (Figure 4-3A to D and F). On the other hand, it seems like that we can detect a prolonged positive hip response to the perturbations that is only slightly affected by the phase shift response (Figure 4-3E). The reason behind this is that the perturbations has two effects: the displacement of the body as a whole and a phase resetting. In this case, the magnitude of the  $\phi$ IRF due to the phase is smaller for the hip compared to the ankle and knee; as a result, the lasting effect of the perturbation can be detected here. However, this effect is concealed by the phase  $\phi$ IRF in the other cases.

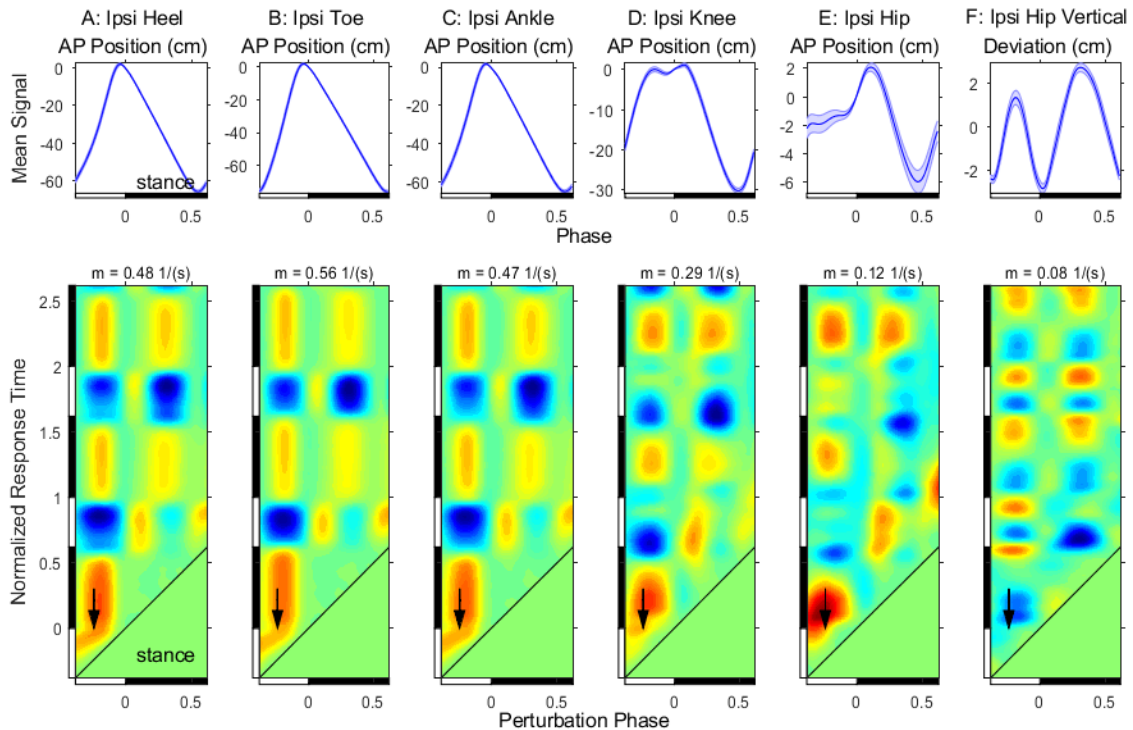


Figure 4-3) Ipsilateral lower body marker displacement response to the mechanical perturbation. AP positions: A. Heel, B. Toe, C. Ankle, D. Knee, E. Hip and F. hip vertical deviation. Above each  $\phi$ IRF is the mean periodic waveform of the response signal with errors bars indicating 95% confidence intervals based on *t*-tests. For vertical ipsilateral hip position, we subtracted the mean from the periodic waveform of each subject before averaging across subjects.

The aforementioned lower body displacements cause changes in joint and segment angles. As mentioned in the methods section, each segment angle measures the upper end movement relative to the lower end, and each joint angle measures the changes in the upper segment angle relative to the lower one. The angular responses here were

similar across different lower body segments and joints. We detected an instantaneous negative response to the perturbations applied during swing phase (indicated by black arrows in Figure 4-4). In other words, when the motor moves forward during swing, we see an instantaneous decrease in joint and segment angles, demonstrating that the lower end moves further forward relative to the upper one.

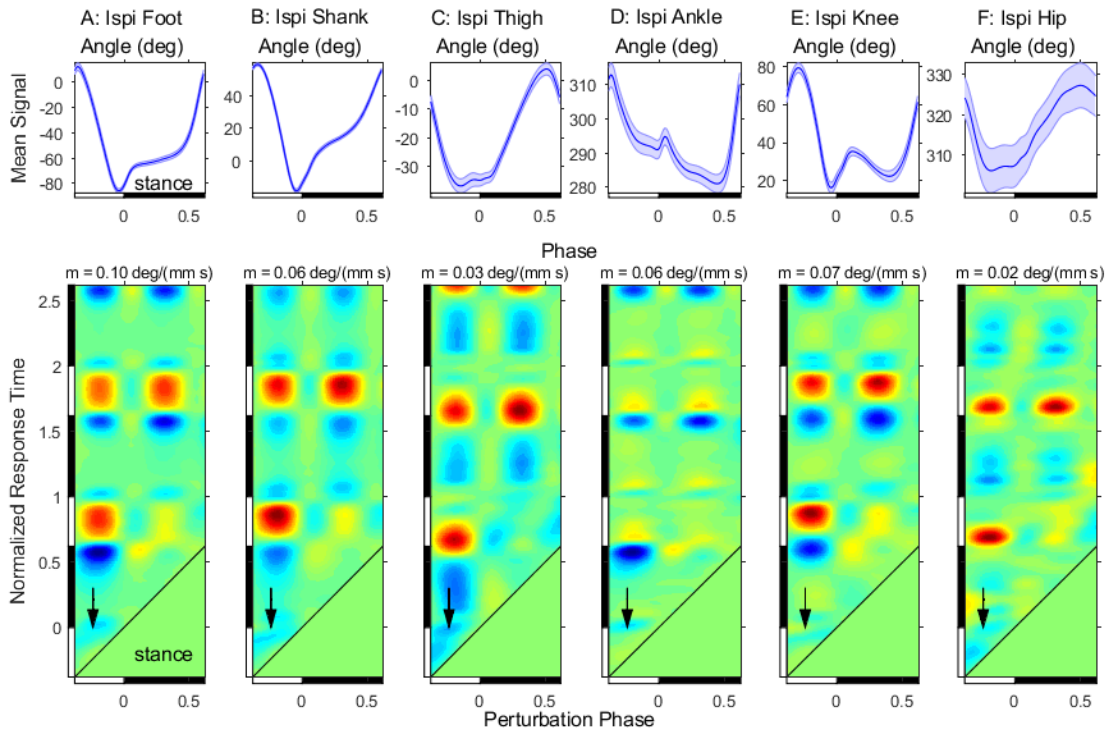


Figure 4-4) Ipsilateral lower body segment (A to C) and joint (D to F) angle response to the mechanical perturbation. A. Foot B. Shank C. Thigh D. Ankle E. knee and F. Hip. Above each  $\phi$ IRF is the mean of the response signal with errors bars indicating 95% confidence intervals based on  $t$ -tests.

For the upper body responses to the mechanical perturbations (Figure 4-5), we considered the AP position of the mid-point between the hip markers (our measure of a subject's position on the treadmill), the AP position the mid-point between the shoulder markers, and the sagittal-plane angle formed by the two mid-points. Position on the treadmill showed an initial positive transient response for perturbations applied during swing and mid stance (Figure 4-5A). On the other hand, the shoulder experienced an initial negative  $\phi$ IRF for perturbations at these periods (Figure 4-5B). These responses together produce the transient negative response in the mid-line trunk

angle (Figure 4-5C). In other words, when the motor moved forward during swing or mid stance, the subject moved forward on the treadmill, with his/her trunk rotating backward. Notice the right-left symmetry in these variable responses (indicated by the black arrows in Figure 4-5) that causes the response to be identical half a cycle apart, for perturbations applied at phases half a cycle apart.

Comparing to the lower body segment angles, the trunk segment angle has a different response to the perturbations. First, the magnitude of this  $\phi$ IRF is much smaller in this variable comparing to the lower body angles. Second and more importantly, the duration of the response is longer here, with the instantaneous response lasting for half the gait cycle. This suggests that the nervous system, for some reason, does not correct for trunk rotation as fast as it does for the other segment angles.

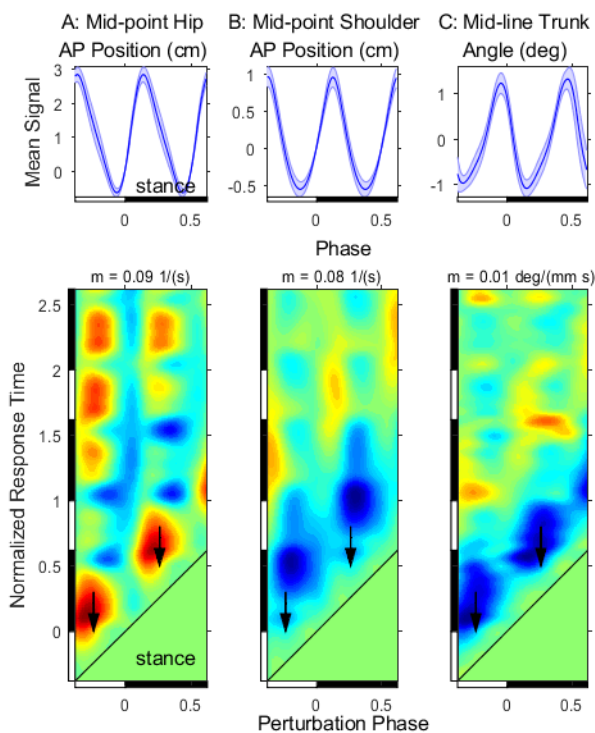
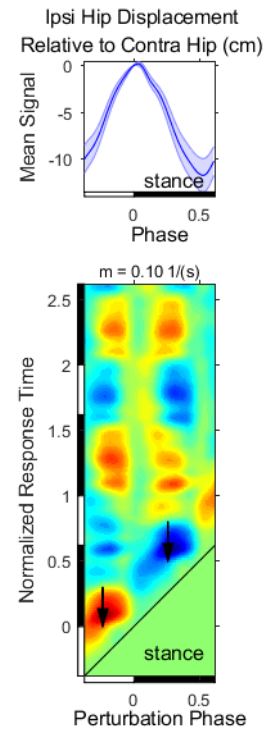


Figure 4-5) Mid-point hip (A.) and shoulder (B.) AP position and mid-line trunk angle (C.) response to the mechanical perturbation. The mean trunk signal with errors bars indicating 95% confidence intervals based on *t*-tests is depicted above the  $\phi$ IRF.

Lastly, we analyzed the pelvis yaw in the transverse plane. We used the ipsilateral hip marker displacement relative to the contralateral hip marker as a measure of yaw. Figure 4-6 illustrates how this variable responds to the mechanical perturbation. The pelvis yaw initially responds to perturbations applied during swing in the same direction as the perturbation, that is, when the motor moves forward during swing, the ipsilateral hip rotates forward relative to the contralateral hip. Of all the kinematic variables we considered, hip rotation is the only one that has skew left-right symmetry, which means that it changes sign when left and right are switched. For the  $\phi$ IRF for a response variable with skew left-right symmetry (e.g., Figure 4-6), if the perturbation phase is delayed by half a cycle, then the response changes sign and is also delayed by half a cycle.

Figure 4-6) Ipsilateral hip displacement relative to contralateral hip response to the mechanical perturbation. The mean of the response signal with errors bars indicating 95% confidence intervals based on  $t$ -tests is depicted above the  $\phi$ IRF



#### EMG Responses to the Mechanical Perturbation

EMG data were collected from 14 muscles, and the data presented in this section illustrate the behavior of the muscles with significant responses to the mechanical perturbation (total of 12). Unlike the kinematic responses, which showed an instantaneous response to the perturbation, the muscular responses happened after some delay and were more phase specific. In all cases, the changes in the EMG activation levels for each muscle were detected at phases of the gait cycle at which the muscle was normally active. These transient responses were followed by responses due to the phase delay. Here we go through the specifics of these behaviors based on the timing of muscle responses, as indicated by the headings below. We also recall key features of the kinematic responses to the perturbation described above, since based on joint input-output inference, the kinematic responses caused the EMG responses.

##### *Late swing:*

The first muscular response was detected during late swing. Recall that forward movement of the motor during early to mid-swing caused the foot to move forward

(Figure 4-3A to C), the knee to extend (Figure 4-4E), and the hip to flex (Figure 4-4F). After a short delay, the kinematic responses caused increased activity during late swing in hamstring muscles (yellow arrows in Figure 4-7E and F), which are normally active during late swing. Both muscles act to flex the knee and extend the hip. Thus, their increased activity is consistent with stretch reflexes that potentially correct the kinematic effects of the perturbation. Supporting this view, when the motor moved forward during early swing, the forward response of the foot is at least partially corrected by the beginning of stance (Figure 4-3A to C).

### *Heel strike and early stance:*

This period is an important phase of gait, during which several muscle groups work together. The dorsiflexor muscles are the first group to activate during this period in normal walking, and here the initial response to the motor displacement was detected in tibialis anterior (Figure 4-7D). Perturbing the ankles forward during swing caused the tibialis anterior to respond in early stance, right after heel strike, by increasing its activation. This finding is consistent with the idea that the nervous system uses tibialis anterior for regulating the propulsion [Kiemel et al., 2016]. When forward motor movement causes the body to move forward, the amount of this forward displacement is greater for the foot than for more proximal body segments such as the pelvis (Figure 4-3). As a result, the nervous system may increase the activation of the tibialis anterior muscle to help the pelvis to catch up with the stance foot.

The next muscle groups that responded to the swing phase perturbation were calf muscles, which decreased their activation in early stance (indicated by the pink arrows in Figure 4-7A and C). The calf muscle responses seemingly last as long as the dorsiflexor response is present. The timing of these responses suggests that the negative transient response in the plantarflexor muscles might be partially caused by reciprocal activation. Decreasing the calf muscle group activation might contribute to leg propulsion.

The quadriceps and gluteus medius are the other muscles that are active during early stance. These muscles groups show similar behavior (Figure 4-7G to J). They both experience an increase in their activity level during early stance in response to perturbations applied during the swing phase. The quadriceps muscles group are thought to be active during this period in order to bend the knee during early stance [Boakes and Rab, 2006], and the gluteus muscles activation during this period can help rotate the thigh forward. As the result, both of these responses contribute to forward progression of the body, which explains why the nervous system might increase their activity.

The quadriceps' antagonistic muscle group, the hamstrings, also show a reciprocal activation behavior. In response to forward perturbations applied during swing,



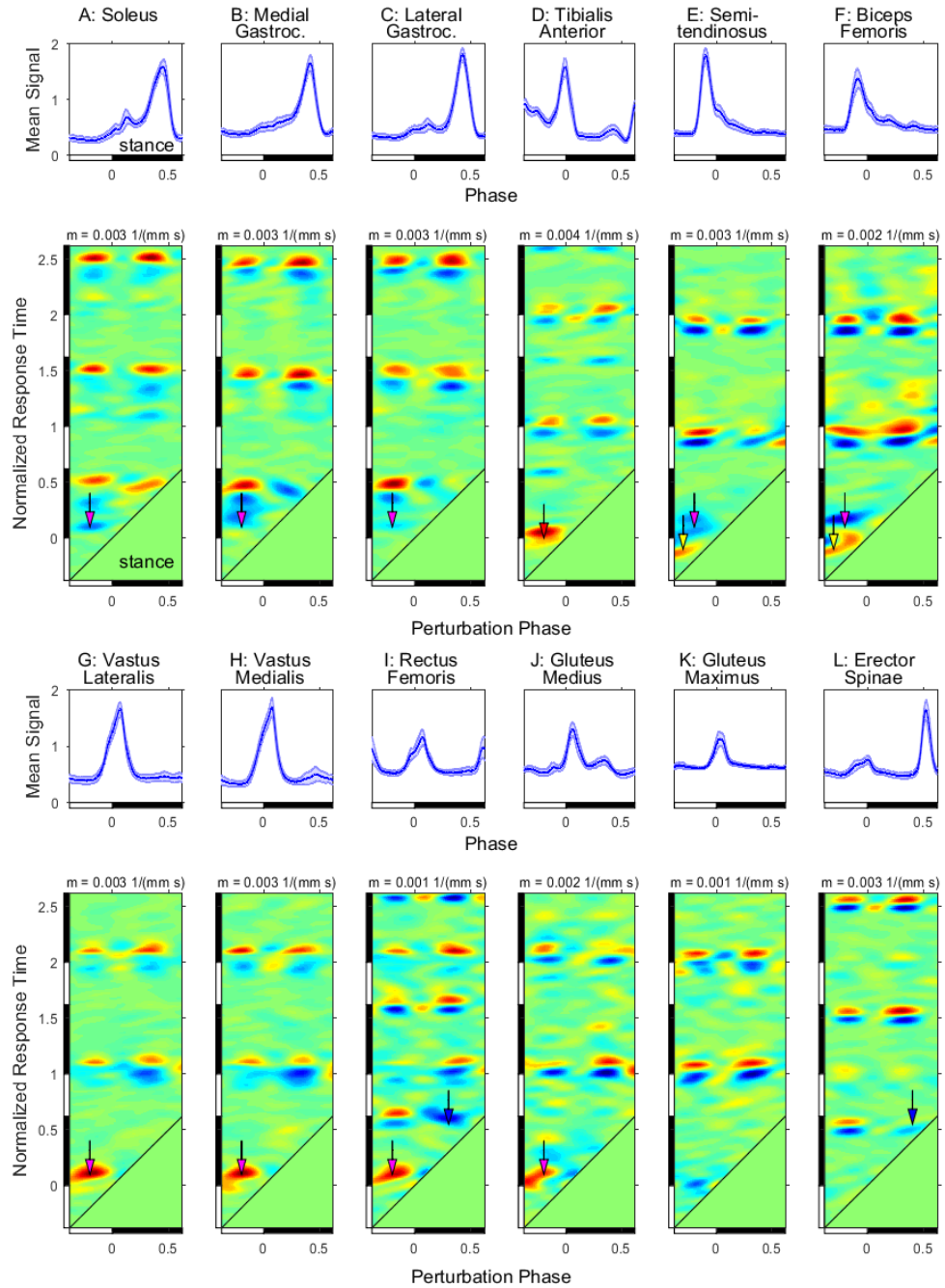


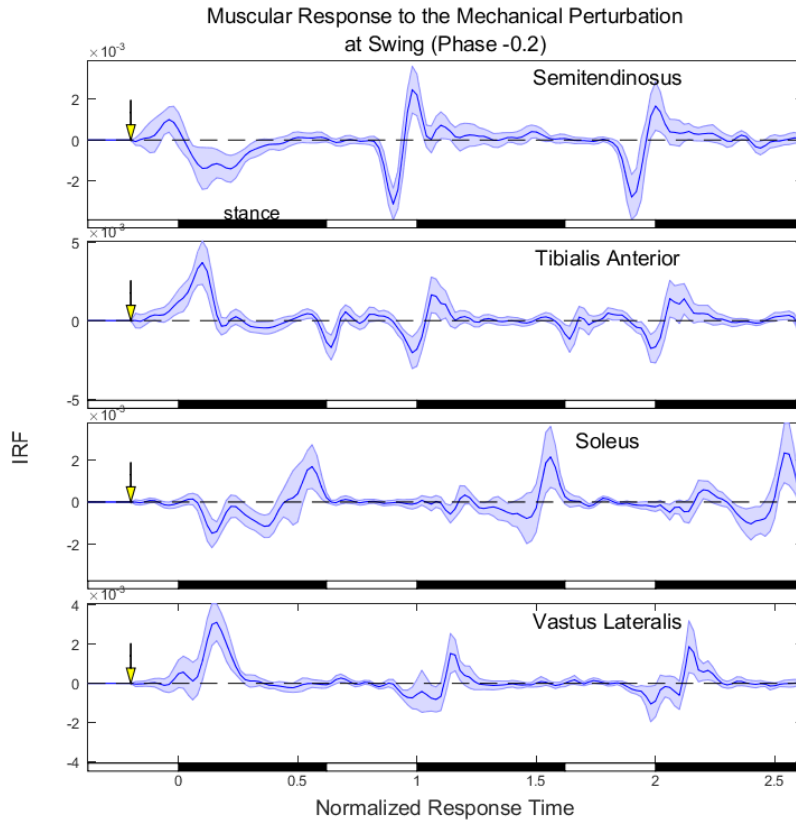
Figure 4-7) Ipsilateral leg (A. to D.), thigh (E. to I.), gluteal (J. to K.) and back (L.) muscle response to the mechanical perturbation. Above each  $\phi$ IRF is the mean of the response signal with errors bars indicating 95% confidence intervals based on  $t$ -tests.

hamstring activation decreases around the same time that quadriceps activation increases (indicated by the pink arrows in Figure 4-7E and F).

In general the strategies found here to stabilize walking in early stance phase are similar to those reported by Kiemel et al. [2011] in a posture study in which they showed that to move the pelvis forward during standing, the nervous system decrease the activity of posterior muscles and increases the activity of anterior muscles.

*Late stance and early swing:*

Erector Spinae is normally active during late stance, probably in order to counteract the unbalancing hip acceleration that is caused by the other leg's heel strike [Winter, 1995]. As the results, we were able to detect changes in activation levels of this muscle in this period. Erector Spinae showed significant negative response for perturbations applied during mid stance (Figure 4-7L). This decrease in activation when the motor moved forward can be explained by the muscle's action to rotate the trunk backwards. Recall that the mechanical perturbation has caused the trunk to rotate backward (the



negative response in Figure 4-5). In order to correct for this rotation, the Erector Spinae activation should be decreased.

*Figure 4-8) Mean  $\phi$ IRF of ipsilateral muscles to mechanical perturbation applied at phase  $t_s = -0.2$  with errors bars indicating 95% confidence intervals based on  $t$ -tests.*

Rectus Femoris is the other muscle known to be normally active during late stance and early swing. It has been suggested that the muscle activation in this period contributes to cadence [Boakes and Rab, 2006]. Here, we observed that Rectus Femoris decreased its activation level during late stance to early swing in response to perturbations applied during mid stance (Figure 4-7I). This finding is consistent with the role of rectus femoris in regulating cadence. As mentioned earlier, the mechanical perturbation, during swing causes phase delay in treadmill walking. The decrease in the rectus femoris activation might contribute to a decrease in cadence and, thus, a phase delay in the gait cycle.

Figure 4-8 shows the timing of different muscle group responses to the mechanical perturbations applied during swing at phase -0.2.

### Sensory Perturbation

The main focus of this study was to better understand the human walking response to mechanical perturbations at the ankle level. For the sake of comparison, we have also studied the system response to sensory perturbations, which were applied simultaneously with the mechanical perturbations. The sensory perturbation signal was the visual scene rotational velocity in units of deg/s, where forward rotation away from the subject was considered positive. Thus,  $\phi$ IRFs describe inferred responses to small impulses in visual-scene velocity, which are equivalent to the responses to small step changes in visual scene position away from the subject. According to joint input-output inference, the EMG responses to a sensory perturbation cause the kinematic responses as described by the plant (Figure 1-1), including phase resetting. According to short-latency inference, if we assume that subjects interpret forward rotation of the visual scene as slowing in their walking speed, the initial EMGs responses describe how neural feedback would respond to actual undesired slowing in walkin speed. In this section, we briefly review these responses and compare the behavior of the system to mechanical and sensory perturbations.

## Phase Response to Sensory Perturbations

Contrary to the phase response of the system to the mechanical perturbation, here we detected a phase advance in response of the system to the sensory perturbation. Figure 4-9 depicts the estimated phase response to the visual perturbation. The positive  $\phi_{IRF}$  in this figure means that when the visual scene rotates 1 degree forward and stays there, at any phase of the gait cycle, the system experiences a phase advance that persists thereafter.

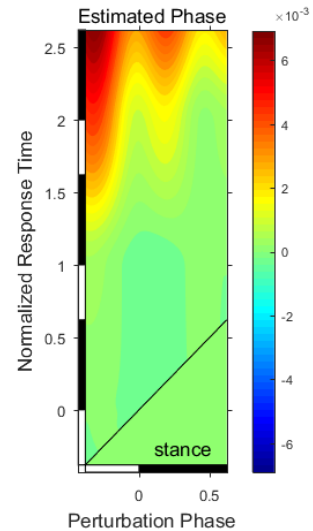


Figure 4-9) Estimated phase response to the visual perturbation

## EMG Responses to Sensory Perturbations

The visual perturbations evoked muscular responses, presumably because movement of the visual scene creates an illusion of self-motion in the opposite direction. Similar to the muscular responses to the mechanical perturbations, the muscular responses detected here were phase dependent. In addition, responses of some muscles were similar for the sensory and mechanical perturbations, especially in when the perturbations were applied during the swing phase. We expected to see some similarities in the muscular responses between these two classes of perturbations. This would suggest that in response to various perturbations the nervous system uses the same general control strategy to maintain stability. On the other hand, we expected to see some differences, since in the case of a sensory perturbation there is an illusion of self-motion, whereas in the case of a mechanical perturbation the subject has been actually moved. In addition, the differences in the behaviors of some muscles can be due to the fact that, unlike the mechanical perturbation, a visual perturbation applied during stance can affect muscle activations. In this section we go through the muscular behaviors based on the timing of the detected responses, as indicated by the headings below.

*Heel strike and early stance:*

The muscular behavior here was similar to what we observed in response to the mechanical perturbations. In response to forward visual-scene rotation during the swing phase, the dorsiflexor muscle Tibialis Anterior showed increased activity right after heel strike (indicated by the red arrow in Figure 4-10D). Here again we suggest

that the activity of tibialis anterior is modulated in order to regulate propulsion. When the visual-scene rotates forward, the subject perceives he/she has moved in the opposite direction and he/she tries to speed up; as a result, the nervous system activates the tibialis anterior to reach that end.

Similar to their behavior in response to the mechanical perturbations, the plantarflexors showed decreased activity in early stance (indicated by the pink arrow in Figure 4-10A to C), which can be explained by reciprocal activation.

Finally, the knee extensors and gluteal muscles showed similar behavior during early stance in response to both classes of perturbations; they experienced an increase in activation (indicated by the pink arrow in Figure 4-10G to K). This behavior can again be explained by the role that these muscles play at this phase in body progression, when the leg is moved forward and the rest of the body needs to catch up.

*Late stance:*

On the other hand, for late stance responses, the muscular behavior was not similar to the system response to mechanical perturbation. Here the plantarflexors showed increased activity at late stance, for perturbations applied in early stance (indicated by the blue arrow in Figure 4-10A to C). These muscles are thought to be active in mid and late stance in order to keep the knee extended, which would allow the body to “fall forward” with little energy cost [Boakes and Rab, 2006]. The reason that we see this mechanism used here, but not in response to the mechanical perturbation, is that the sensory perturbation, unlike the mechanical perturbation, was effective when applied during the stance phase. The nervous system looks for a strategy that corrects perturbations as soon as possible and uses the knee extensor muscles that are already active.

We also observed that Rectus Femoris and Erector Spinae experienced increased activity in late stance to perturbations applied in mid stance (indicated by the blue arrow in Figure 4-10I and L). For rectus Femoris, the difference of the muscle activation in response to these two classes of perturbations, can be again explained by the role that early stance modulation of rectus femoris plays in regulating cadence. As mentioned earlier, in response to the visual perturbation, the system experiences a phase advance, which is consistent with the increased activation of rectus femoris.

As for the erector spinae, when the visual scene rotated forward during mid stance, this muscle first showed a decrease in activation at late stance, followed by an increase in activation, which presumably contributed to the forward rotation of the trunk (look at the kinematic response to the visual perturbation in Figure 4-11). There are at least two reasons why the nervous system might act to rotate the trunk forward: 1) the forward rotation of the visual scene is interpreted as backward rotation of the trunk;

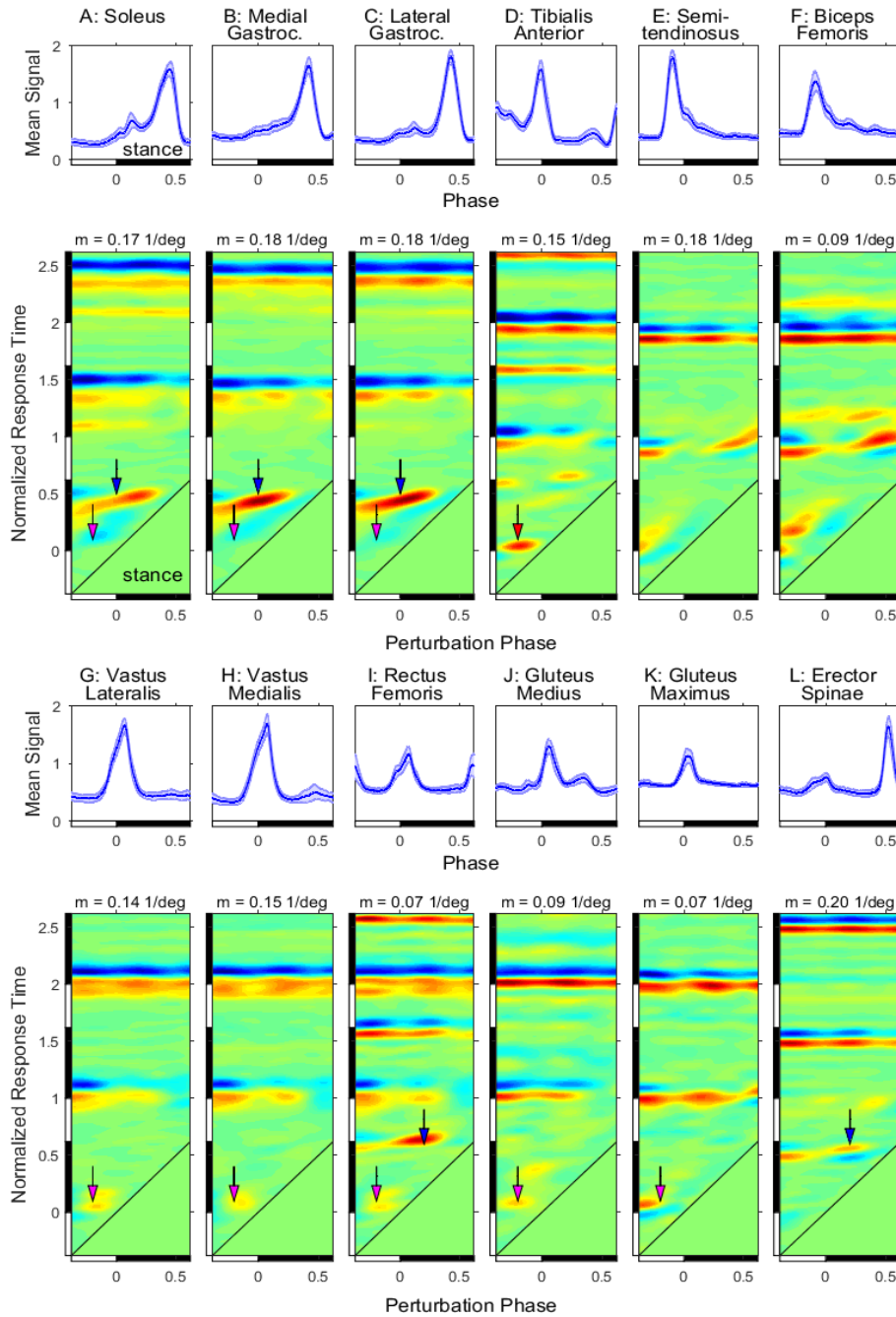


Figure 4-10) Ipsilateral leg (A. to D.), thigh (E. to I.), gluteal (J. to K.) and back (L.) muscle response to the visual perturbation. Above each  $\phi$ IRF is the mean of the response signal with errors bars indicating 95% confidence intervals based on  $t$ -tests.

and 2) forward rotation of the visual scene is interpreted as an undesired slowing in walking speed and forward trunk rotation anticipates forward acceleration of the pelvis (see [Logan et al., 2017] for more details). In either case the nervous system would be expected to increase erector spinae activation.

The effect of the phase advance can be detected in the muscular responses as well. Figure 4-10 Figure 4-13 shows that all the transient responses are followed by the successive red and blue bars which indicate the phase advance effect on muscular behavior.

### Kinematic Responses to Sensory Perturbations

According to joint input-output inference, changes in muscular activity cause changes in position and velocity. Using the midpoint of the two hip markers as an indicator of the person's position on the treadmill, we studied the AP velocity response to the sensory perturbations (Figure 4-11A). We observed that the visual perturbations cause a delayed positive response for perturbations applied at any phase of the gait cycle. In other words, when the visual scene rotates forward, the subjects increase their speed in order to catch up. Unlike the velocity response to the mechanical perturbation, the positive response here lasts for almost an entire cycle.

The increase in walking velocity in response to forward visual-scene rotation produced a long-lasting forward shift in a subject's position on the treadmill (Figure 4-11B). The initial delayed positive response here means that when the visual scene rotates forwards at any phase of the gait cycle and stays there, the subject moves forward as well after a delay. Contrary to the responses to the mechanical perturbation, here the response lasts thereafter, which is due to the nature of perturbation. Similar behavior has been detected for the other lower body AP positions.

Preceding forward response of the subject's position on the treadmill, the trunk angle exhibited a delayed forward rotation in response to forward visual-scene rotation at any phase of the gait cycle (Figure 4-11D). This was accompanied by a delayed forward displacement of the shoulders (Figure 4-11C). Recall that, in contrast, the mechanical perturbation caused backward shoulder displacement and backward trunk rotation. Much like the AP velocity response, the trunk midline angle response lasts for almost an entire cycle.

In summary, there are three main differences in the kinematic responses to the visual perturbation compared to the mechanical perturbation: 1) the responses occur after a delay; 2) they are present for perturbations applied at any phase of the gait cycle; and 3) the transient responses, in general, last longer.

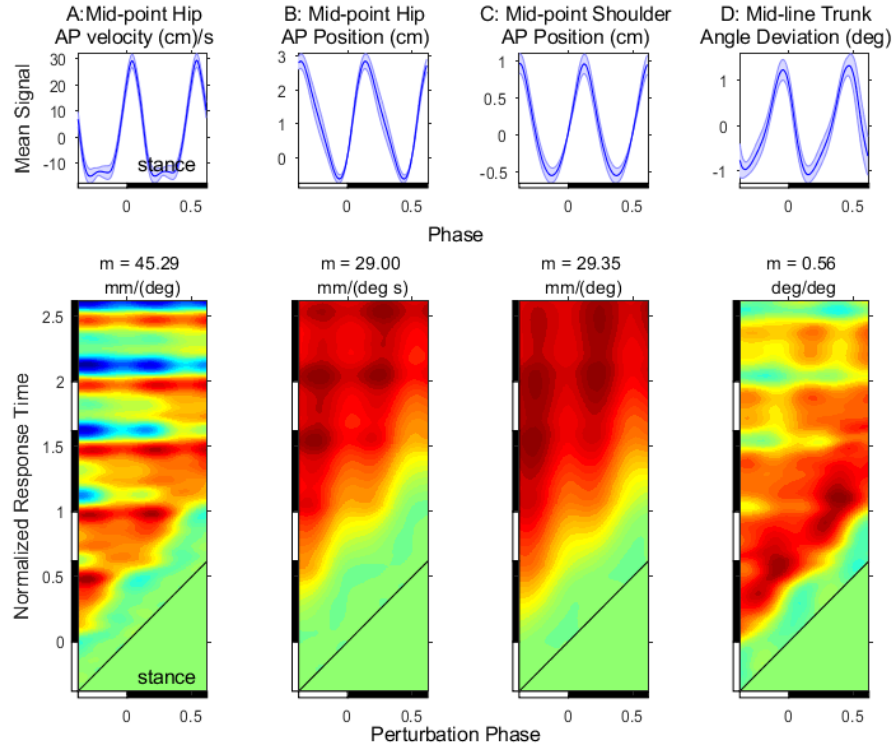


Figure 4-11) Kinematic response to the visual perturbation. A. mid-point hip AP velocity B. mid-point hip AP position C. mid-point shoulder AP position D. Mid-line trunk angle deviation. Above each  $\phi$ IRF is the mean of the response signal with errors bars indicating 95% confidence intervals based on  $t$ -tests.

#### Comparing Perturbed and Unperturbed Mean Waveforms

Finally, in order to analyze how the perturbations affected normal human walking, we compared the mean waveform obtained from different condition for all variables. As mentioned in the methods section, in the first and last trials the subjects did not wear the ankles supports and did not experience any perturbation (*Unattached* condition). In addition, there were 10 s windows at the beginning and end of the perturbed trials during which the motor and the visual scene were stationary (*Stationary* condition). Taking into account the perturbed time windows (*Perturbed* condition), there were three different conditions that were compared. To compare the mean waveform patterns among these conditions, for each kinematic or EMG variable, we computed the root mean square (RMS) difference between the Stationary and Unattached conditions and between the Perturbed and Unattached conditions.



Kinematic waveforms were similar for all three conditions. For segment angles, the RMS differences were at most 0.783 deg (Fig. 4-12 for foot angle). For AP positions, RMS differences were at most 0.4 cm. These small differences were consistent with the participants' subjective experience; subjects reported that after the familiarization period, they did not notice any particular change in their walking style due to the perturbation apparatus or the perturbations themselves.

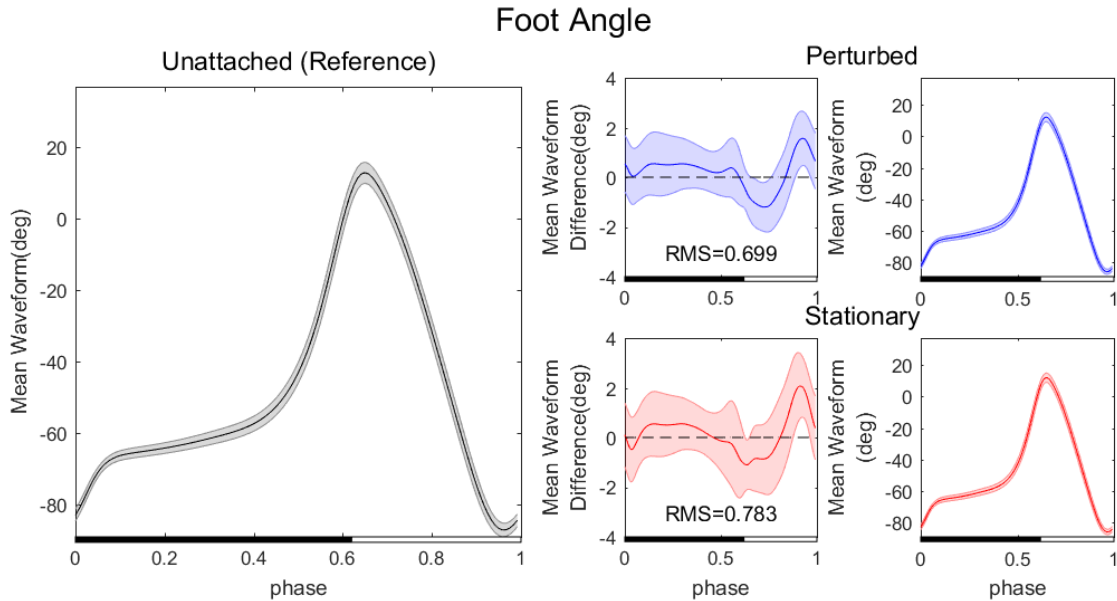
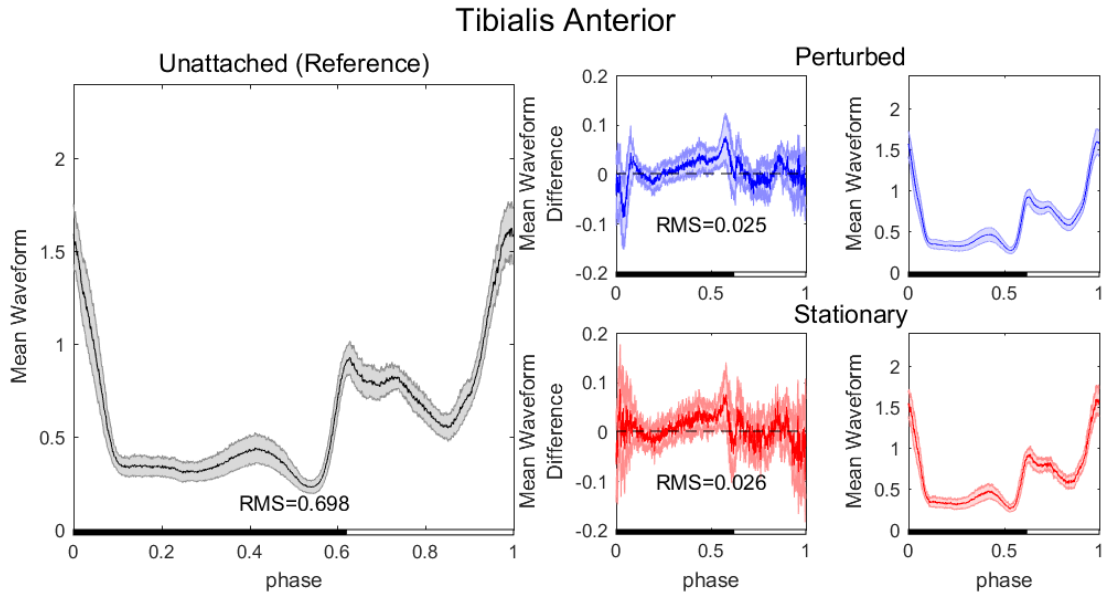


Figure 4-12) Comparison between the foot angle mean waveform in different conditions (unattached, stationary and perturbed). The mean waveforms are depicted with errors bars indicating 95% confidence intervals based on *t*-tests

Small differences among conditions were also found for EMG mean waveforms, which were qualitatively similar for all conditions. The ratio of the RMS difference to RMS of the mean Unattached signal was at most 0.06 (rectus femoris). To illustrate typical results for EMG data, Figure 4-13 compares the shape of the mean waveform for the tibialis anterior signal in these different conditions.



*Figure 4-13) Comparison between the Tibialis Anterior mean waveform in different conditions (unattached, stationary and perturbed). The mean waveforms are depicted with error bars indicating 95% confidence intervals based on *t*-tests*

In summary, although mechanical perturbations affected mean kinematic and EMG waveforms, deviations were small and in most cases, they resembled variance in gait pattern observed between different subjects. Therefore, we conclude that the properties of the neural control of walking identified in this study using our weak mechanical perturbation are likely similar to the properties of neural control during unperturbed walking.

## Chapter 5 : Discussion

The objective of this study was to investigate the response of human walking to mechanical perturbations at ankle level, in order to investigate the role of strategies that stabilize walking. For the sake of comparison, we also studied the human walking response to a sensory perturbation, movement of a virtual visual scene. In the results section, we showed that the mechanical perturbations produced kinematic responses (Figure 4-2 to Figure 4-6), which illustrates that our method of perturbing gait was effective. In addition, we reported muscular (EMG) responses to the applied

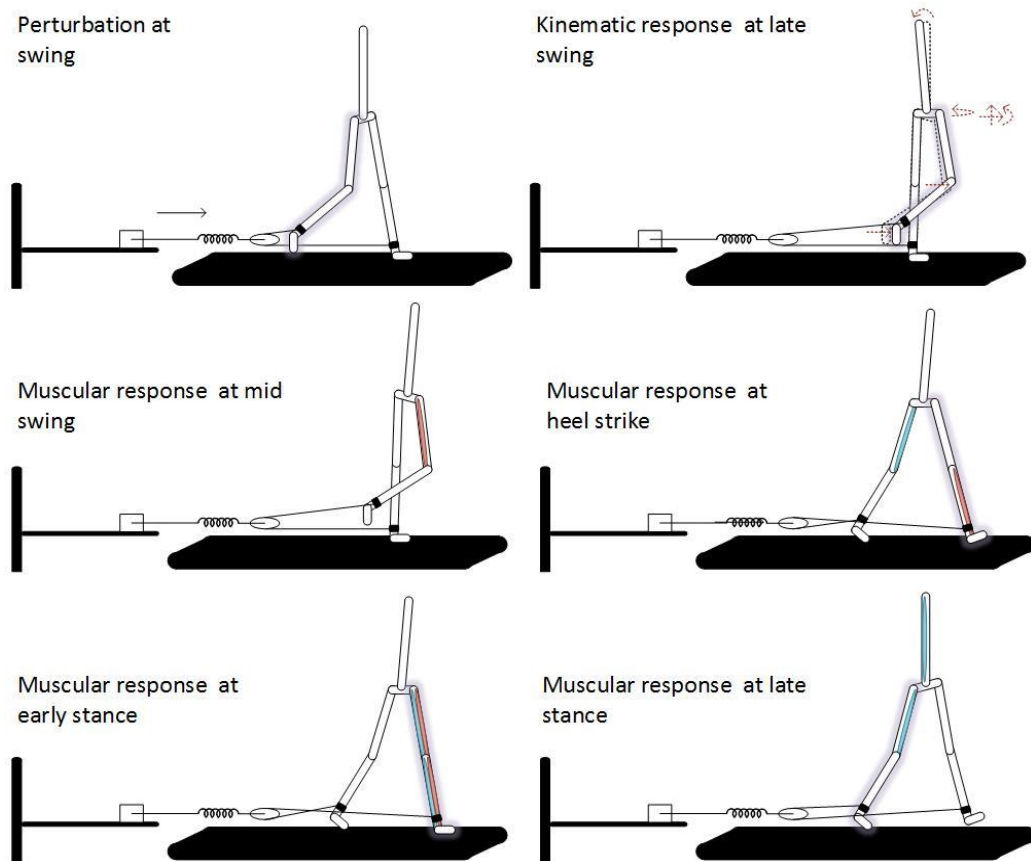


Figure 5-1) Stick figures that illustrate the kinematic and muscular response of human walking to a mechanical perturbation applied during mid-swing. The dashed figure in late swing represents unperturbed kinematics. Muscle activation is color coded: blue indicates decrease in activation and red indicates increase.

mechanical perturbations (Figure 4-7), indicating that neural feedback contributed to stabilizing gait. All responses were highly dependent on the phase at which the perturbations were applied, and muscular responses occurred at characteristic phases of the gait cycle. Figure 5-1 illustrates the kinematic and muscular response of human walking at different phases of gait cycle to mechanical perturbations applied in the swing phase. The perturbation shown here is positive (forward movement of the motor), and the muscle group activation is color-coded with red indicating an increase in activation and blue indicating a decrease. This figure illustrates that the response to the mechanical perturbations first occurs in kinematics and then later on in different muscle groups. In this chapter, we further discuss the initial open-loop responses and the later active control strategies implemented by the nervous system in order to correct for the deviations from the normal pattern.

### Open-loop Responses

Initial transient kinematic responses before the minimum time delay of neural feedback were necessarily open-loop and determined by inertial and viscoelastic properties of the body. In response to backward motion of the motor during mid-swing, the trunk (Figure 4-5C) and ipsilateral thigh and shank segments (Figure 4-4B and C) rotated in the clockwise direction with the shoulder moving forward (Figure 4-5B) and all levels of the ipsilateral leg moving backwards (Figure 4-3). The fact that the kinematic variables showed instantaneous responses to the perturbations (Fig 5-2, top row) indicates the open-loop nature of these responses. It would have taken in order of 40-50 ms for the fastest active control strategy (the short-latency stretch reflex response in this case) to act on the system [Grey et al., 2004; Jones and Watt, 1971]. The fact that the initial kinematic response is a ramp ( $\phi_{IRF} h(t_r, t_p) \propto t_r - t_p$ ) rather a step or quadratic function is consistent with how a system with inertia and viscoelastic properties responds to an impulse of force (see Appendix B). To further illustrate this point, Figure 5-2 compares the transient responses to the mechanical perturbation of a kinematic variable (ipsilateral ankle AP position), and muscular variable (EMG of tibialis anterior), whose initial response is not statistically significant.

Note the small variability for ankle AP position during roughly the first 100 ms (Figure 5-2, top row), indicating similar initial open-loop kinematic responses near the point where the perturbation was applied. Variability started to increase at about 100 ms, which is when the effect of neural feedback (long-latency stretch reflex) becomes evident. This suggests that there were quantitative differences in neural feedback across subjects. After heel strike, variability remained roughly constant, since the foot was on the ground afterwards. In contrast, the initial small variability was not present in other kinematic responses or the EMG responses. Notice that the Tibialis Anterior activation

(Figure 5-2 bottom row) does not start with a small variability, reflecting the variability of active control and/or the variability in its measurement. So, what can be said about the active control?

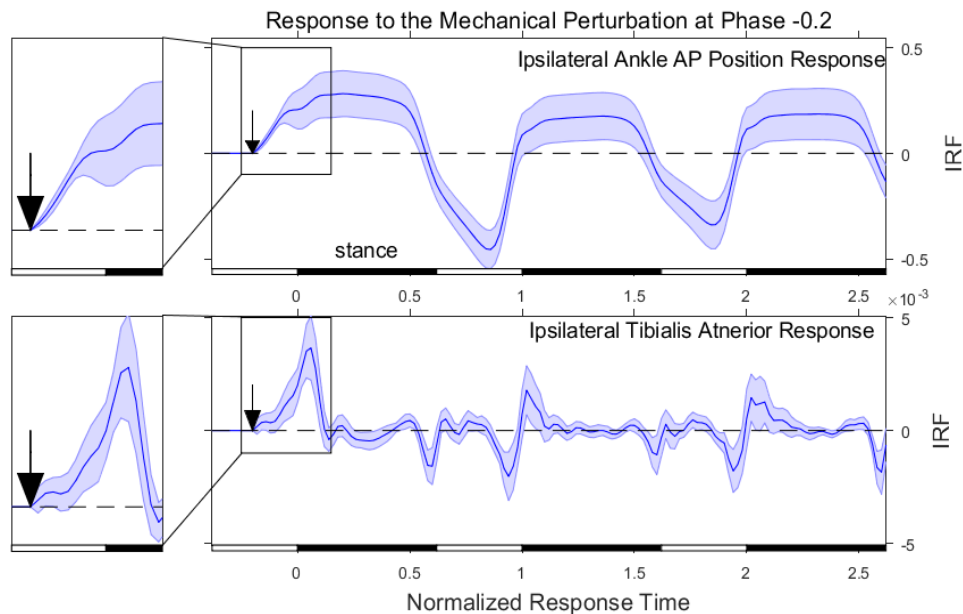


Figure 5-2) Comparison between the shape of the kinematic and muscular transient response to mechanical perturbation.

### Feedback Responses

To maintain stability, the system had to correct for the perturbations using various control strategies. The fact that kinematic responses resulted in delayed EMG responses and a delay in the phase of the gait cycle both indicate that neural feedback contributed to correcting the kinematic deviations.

We found that two different strategies can be used by individual muscle groups in order to assist the system. Muscle groups can be activated simply to oppose the passive kinematic responses (similar to reactive strategies), or they can use more complex control strategies such as anticipatory control that compensate for the kinematic responses. The strategy that the individual muscle groups use, primarily depend on the state of the foot on the ground (stance phase vs. swing phase). The muscular responses that were used to correct perturbations in the swing phase, had reactive characteristics. For instance, we saw that the hamstring muscles showed increased activity shortly after the forward movement of the motor to correct of the extension of the knee and flexion of the hip. Recall from the results section that the forward movement of the motor

displaced the foot forward relative to the pelvis (Figure 4-3). As a result, the nervous system activated the hamstring muscles, presumably by a long-latency stretch reflex mechanism, to partially correct for the extension of the knee. Similar strategy has been reported in the literature for larger perturbations; Eng et al. [1994] established the role of the hamstring muscle group in regression of the leg during late swing as a recovery strategy for tripping. Another example of a reactive control strategy involves the erector spinae, which, in response to a forward mechanical perturbation at the ankle, decreased its activity in order to correct for the trunk backward rotation. Recall that positive mechanical perturbations cause the trunk to rotate backward (Figure 4-5C). In response to this behavior, the erector spinae, which is responsible for bending back the trunk, decreases its activation level, in order to help rotate the trunk forward to its upright position.

On the other hand, if the kinematic deviation produced by a mechanical perturbation during swing was not completely corrected by the time of foot placement, then a simple reactive control strategy no longer sufficed to correct the kinematic deviation. Instead, the strategies that were used in the stance phase were anticipatory and compensated for the kinematic responses in the coming cycles of movement. Most muscular responses to the mechanical perturbation that we detected belonged in this category, including the response of tibialis anterior muscle. As mentioned earlier, forward motor movement during swing caused the next foot placement to be displaced in the forward direction, and the amount of this forward foot displacement was greater than that of more proximal body segments (Figure 4-3). This response presumably created the need for the pelvis to catch up with placement of the foot. As a result, the tibialis anterior muscle activated in early stance to help the forward progression of the pelvis. Therefore, we can conclude that, it is not just the reflexes that contribute to AP stability [O'Connor and Kuo, 2009], but rather the nervous system uses sensory feedback for anticipatory control strategies such as phase resetting.

In addition, our findings are consistent with the idea that in response to sensory information the nervous system modulates muscles activation at the phases during which the muscles are usually active [Logan et al., 2017]. Therefore, it can be concluded that nervous system does not only stabilize walking through push-offs and collisions. Based on the collision-based models of human locomotion (e.g. [Kuo, 2007] or [Srinivasan and Ruina, 2006]), we would expect the system to enforce control at the next heel strike or push-off. In contrast, our data suggests that even though those time points are important, the nervous system will act earlier, if possible, by modulating the activity of muscles that are normally active at other phases of the gait cycle. Nonetheless, the nervous system does not activate muscles when they are normally silent in response to small perturbations, as it does for larger ones. For instance, in case

of obstacle avoidance, Patla et al. [1991] found that rectus femoris activates in mid swing (when in unperturbed gait is normally silent), to help flex the hip and avoid hitting the obstacle. The question why the system does not behave this way in face of small perturbations, might be addressed by looking at the principals of optimal feedback control [Todorov, 2004]. From this perspective, where motor and sensory noise is present, the optimal controller takes the uncertainty into account to solve the locomotion control problem. In this study, we attempted to identify aspects of this controller.

Finally, comparing muscular responses to the mechanical and sensory perturbations helped us better understand the strategies used by the nervous system for subtask control. We observed similar responses to both forward motion of the visual scene during swing and a mechanical perturbation during swing that caused a forward deviation in foot placement. Both perturbations resulted in increased activation of the ipsilateral tibialis anterior and quadriceps muscles in early stance, followed by forward acceleration of the pelvis. These results suggest a general mechanism of early-stance neural control of walking that is used to accelerate the pelvis relative to the foot to correct various kinematic deviations. In the case of the mechanical perturbation, the pelvis is accelerated forward to catch up with foot. In the case of the sensory perturbation, the pelvis is accelerated forward to correct an illusory slowing in walking speed caused by forward visual-scene motion. In contrast to the similar early-stance responses, contralateral rectus femoris activity during the stance-to-swing transition increased in response to the sensory perturbation and decreased in response to the mechanical perturbation. These results are consistent with the presumed role of rectus femoris in controlling cadence, since the sensory perturbation produced a phase advance in the gait cycle, whereas the mechanical perturbation produced a phase delay.

### Conclusion

In conclusion, gait research has identified critical phases of the gait cycle when the nervous system modulates muscle activity based on sensory feedback to control walking, including late-stance modulation of plantarflexors to control push-off and stance-to-swing modulation of rectus femoris to control cadence. This study provides support for an addition to this list, the modulation of anterior leg-muscle activities during early stance. In particular, our results suggest that this early-stance modulation is a general control mechanism that serves multiple functions, including controlling walking speed and compensating for errors in foot placement.

*Future Directions*

As mentioned in the literature review, there are several models of the neural of human locomotion [Dzeladini et al., 2014; Geyer and Herr, 2010; Song and Geyer, 2012; Taga, 1995]. However, little is known about the response of current models to small continuous perturbations. Going forward, we want to see if the models can mimic what happens in experimental data and revise the models as necessary. For example, the model of Song and Geyer [2015], similar to the previous model of Geyer and Herr [2010] only modulates tibialis anterior (TA) activity to ensure foot clearance during swing and prevent excessive plantarflexion of the ankle during stance and does not explicitly modulate TA activity to correct for deviations in foot placement. Therefore, it is unlikely that this model will produce the early-stance modulation in TA activity that we observed when our mechanical perturbation caused a deviation in foot placement.

In this study, we assumed a local limit cycle (LLC) approximation in which if the direction of the perturbation is reversed, then the direction of the response is also reversed and remains the same in magnitude. This approximation is motivated by our choice to use small perturbations. For larger perturbations, the LLC approximation is known to break down. For example, large ankle perturbations have been reported to evoke reflexes with differences latencies depending on whether the perturbation in the plantarflexion or dorsiflexion direction [Grey et al., 2004]. Similarly, the large visual perturbations have been reported to influence the magnitude of the response, with approaching perturbations resulting in greater kinematic responses [Logan et al., 2014]. Therefore, one challenge for future work is to extend the  $\phi$ IRF analysis used in this study to distinguish the response of the system based on the direction of perturbation.



## Appendixes

### Appendix A: Symmetry

Most kinematic responses to the mechanical perturbation reflected a right-left symmetry, which means that the  $\phi$ IRF would be similar at response times half a cycle apart for perturbations applied at half a cycle apart:

$$h_{uy}(t_r, t_s) = h_{uy}\left(t_r + \frac{T}{2}, t_s + \frac{T}{2}\right) \quad (1)$$

where  $T$  is the cycle period. This effect is caused by three properties.

1) **The right-left symmetry of the system including our perturbations.** In mathematical terms, our state equations have left-right symmetry as described by the following equations:

$$\begin{aligned} \dot{x}(t) &= f(x(t), v(t), d(t)) \\ R(f(x(t), v(t), d(t))) &= f(R(x(t)), v(t), d(t)) \end{aligned} \quad (2)$$

where the function  $f$  defines the system,  $x$  is the vector of state variables,  $v$  is the sensory perturbation,  $d$  is the mechanical perturbation, and the mapping  $R$  switches left and right.

2) **Spatiotemporal symmetry.** The periodic solution of human walking has spatiotemporal symmetry. Specifically, shifting time by half a cycle has the same effect as switching right and left:

$$\tilde{x}\left(t + \frac{T}{2}\right) = R(\tilde{x}(t)), \quad (3)$$

where  $\tilde{x}$  is the periodic solution.

3) **Response variable symmetry.** If the response variable  $y = g(x(t))$  has symmetry ( $R(g(x(t))) = g(R(x(t)))$ ), the  $\phi$ IRF will have the characteristics of equation (1). On the other hand, if the response variable has skew symmetry ( $R(g(x(t))) = -g(R(x(t)))$ ), the  $\phi$ IRF will have the following property:

$$h_{uy}(t_r, t_s) = -h_{uy}\left(t_r + \frac{T}{2}, t_s + \frac{T}{2}\right) \quad (4)$$

### Appendix B: Mass-Spring-Damper System Impulse Response

In a mass-spring-damper system the following equation holds:

$$m\ddot{y}(t) = -ky(t) - c\dot{y}(t) + d(t), \quad (5)$$

where  $m$  is the mass of the system,  $y(t)$  is the position as a function of time  $t$ ,  $k$  is the spring stiffness,  $c$  is the damping constant and  $d(t)$  is the external force. Rearranging the equation (5) and taking the Laplace transform we will have:

$$ms^2Y(s) + csY(s) + kY(s) = D(s) \quad (6)$$

$$H(s) = \frac{Y(s)}{D(s)} = \frac{1}{ms^2 + cs + k} \quad (7)$$

where  $H(s)$  is the transfer function. Given that we want to compute the response to an impulse,  $D(s)$  is equal to 1, resulting in:

$$H(s) = \frac{1}{ms^2 + cs + k} \quad (8)$$

The impulse response function  $h(t)$  is the inverse Laplace transform of  $H(s)$ , which has the form:

$$h(t) = \frac{e^{-at} - e^{-bt}}{m(b - a)} \quad (9)$$

where  $a$  and  $b$  are roots of the denominator of the equation (8) Writing the equation (9) as a Taylor series about  $t = 0$  we will have:

$$\begin{aligned} h(t) &= \frac{(1 - at + O(t^2)) - (1 - bt + O(t^2))}{m(b - a)} \\ &= t/m + O(t^2) \end{aligned} \quad (10)$$

Therefore, we expect that initial responses to our mechanical perturbation will have the form of a linear function of time (a ramp), rather than that of a step function or quadratic function of time.

## Bibliography

- Anderson FC, Pandy MG: Dynamic optimization of human walking. *Journal of biomechanical engineering* 2001;123:381-390.
- Aoi S, Ogihara N, Funato T, Sugimoto Y, Tsuchiya K: Evaluating functional roles of phase resetting in generation of adaptive human bipedal walking with a physiologically based model of the spinal pattern generator. *Biological cybernetics* 2010;102:373-387.
- Bendat JS, Piersol AG: *Random data: analysis and measurement procedures*, John Wiley & Sons, 2011.
- Bhargava LJ, Pandy MG, Anderson FC: A phenomenological model for estimating metabolic energy consumption in muscle contraction. *Journal of biomechanics* 2004;37:81-88.
- Boakes JL, Rab GT: *Muscle activity during walking*. Human Walking Lippincott Williams and Wilkins, Baltimore 2006.
- Conway B, Hultborn H, Kiehn O: Proprioceptive input resets central locomotor rhythm in the spinal cat. *Experimental Brain Research* 1987;68:643-656.
- Creath R, Kiemel T, Horak F, Peterka R, Jeka J: A unified view of quiet and perturbed stance: simultaneous co-existing excitable modes. *Neuroscience Letters* 2005;377:75-80.
- Criswell E: *Cram's introduction to surface electromyography*, Jones & Bartlett Publishers, 2010.
- Dietz V: Spinal cord pattern generators for locomotion. *Clinical Neurophysiology* 2003;114:1379-1389.
- Dietz V, Harkema SJ: Locomotor activity in spinal cord-injured persons. *Journal of Applied Physiology* 2004;96:1954-1960.
- Dingwell J, Cusumano J, Cavanagh P, Sternad D: Local dynamic stability versus kinematic variability of continuous overground and treadmill walking. *Journal of biomechanical engineering* 2001;123:27-32.
- Dzeladini F, van den Kieboom J, Ijspeert A: The contribution of a central pattern generator in a reflex-based neuromuscular model. *Frontiers in Human Neuroscience* 2014;8.
- Eng JJ, Winter DA, Patla AE: Strategies for recovery from a trip in early and late swing during human walking. *Experimental Brain Research* 1994;102:339-349.
- Feldman AG, Levin MF: The origin and use of positional frames of reference in motor control. *Behavioral and Brain Sciences* 1995;18:723-806.
- Geyer H, Herr H: A muscle-reflex model that encodes principles of legged mechanics produces human walking dynamics and muscle activities. *Neural Systems and Rehabilitation Engineering, IEEE Transactions on* 2010;18:263-273.
- Geyer H, Seyfarth A, Blickhan R: Positive force feedback in bouncing gaits? *Proceedings of the Royal Society of London B: Biological Sciences* 2003;270:2173-2183.
- Geyer H, Seyfarth A, Blickhan R: Compliant leg behaviour explains basic dynamics of walking and running. *Proceedings of the Royal Society B: Biological Sciences* 2006;273:2861-2867.
- Grey MJ, Mazzaro N, Nielsen JB, Sinkjær T: Ankle extensor proprioceptors contribute to the enhancement of the soleus EMG during the stance phase of human walking. *Canadian journal of physiology and pharmacology* 2004;82:610-616.
- Grey MJ, Nielsen JB, Mazzaro N, Sinkjær T: Positive force feedback in human walking. *The Journal of physiology* 2007;581:99-105.
- Guckenheimer J, Holmes PJ: *Nonlinear oscillations, dynamical systems, and bifurcations of vector fields*, Springer Science & Business Media, 2013.
- Günther M, Ruder H: Synthesis of two-dimensional human walking: A test of the  $\lambda$ -model. *Biological Cybernetics* 2003;89:89-106.

- Hof AL: The 'extrapolated center of mass' concept suggests a simple control of balance in walking. *Human movement science* 2008;27:112-125.
- Holmes P, Full RJ, Koditschek D, Guckenheimer J: The Dynamics of Legged Locomotion: Models, Analyses, and Challenges. *SIAM Review* 2006;48:207-304.
- Horak FB, Nashner LM: Central programming of postural movements: adaptation to altered support-surface configurations. *Journal of neurophysiology* 1986;55:1369-1381.
- Hultborn H, Nielsen JB: Spinal control of locomotion—from cat to man. *Acta Physiologica* 2007;189:111-121.
- Jezernik S, Colombo G, Keller T, Frueh H, Morari M: Robotic Orthosis Lokomat: A Rehabilitation and Research Tool. *Neuromodulation* 2003;6:108-115.
- Jones GM, Watt D: Observations on the control of stepping and hopping movements in man. *The Journal of Physiology* 1971;219:709.
- Kang HG, Dingwell JB: A direct comparison of local dynamic stability during unperturbed standing and walking. *Experimental Brain Research* 2006;172:35-48.
- Kiemel T, Elahi AJ, Jeka JJ: Identification of the plant for upright stance in humans: multiple movement patterns from a single neural strategy. *Journal of neurophysiology* 2008;100:3394-3406.
- Kiemel T, Logan D, Jeka JJ: Using perturbations to probe the neural control of rhythmic movements. arXiv preprint arXiv:160701746 2016.
- Kiemel T, Zhang Y, Jeka JJ: Identification of neural feedback for upright stance in humans: stabilization rather than sway minimization. *The journal of Neuroscience* 2011;31:15144-15153.
- Kuo AD: The relative roles of feedforward and feedback in the control of rhythmic movements. *MOTOR CONTROL-CHAMPAIGN-* 2002;6:129-145.
- Kuo AD: The six determinants of gait and the inverted pendulum analogy: A dynamic walking perspective. *Human movement science* 2007;26:617-656.
- Logan D, Ivanenko YP, Kiemel T, Cappellini G, Sylos-Labini F, Lacquaniti F, Jeka JJ: Function dictates the phase dependence of vision during human locomotion. *Journal of neurophysiology* 2014;112:165-180.
- Logan D, Kiemel T, Jeka JJ: Using a System Identification Approach to Investigate Subtask Control during Human Locomotion. *Frontiers in Computational Neuroscience* 2017;10.
- McFadyen BJ, Winter DA: Anticipatory locomotor adjustments during obstructed human walking. *Neuroscience Research Communications* 1991;9:37-44.
- Möllerstedt E, Bernhardsson B: Out of control because of harmonics—an analysis of the harmonic response of an inverter locomotive. *Control Systems, IEEE* 2000;20:70-81.
- Moore JK, Hnat SK, van den Bogert AJ: An elaborate data set on human gait and the effect of mechanical perturbations. *PeerJ* 2015;3:e918.
- Mori F, Nakajima K, Tachibana A, Takasu C, Mori M, Tsujimoto T, Tsukada H, Mori S: Reactive and anticipatory control of posture and bipedal locomotion in a nonhuman primate; in: *Progress in Brain Research*. 2004, vol 143, pp 191-198.
- Nashner LM: Balance adjustments of humans perturbed while walking. *Journal of Neurophysiology* 1980;44:650-664.
- O'Connor SM, Kuo AD: Direction-dependent control of balance during walking and standing. *Journal of neurophysiology* 2009;102:1411-1419.
- Pai Y-C, Patton J: Center of mass velocity-position predictions for balance control. *Journal of biomechanics* 1997;30:347-354.
- Pang MY, Yang JF: The initiation of the swing phase in human infant stepping: importance of hip position and leg loading. *The Journal of physiology* 2000;528:389-404.

- Patla AE: Strategies for Dynamic Stability During Adaptive Human Locomotion. *IEEE Engineering in Medicine and Biology Magazine* 2003;22:48-52.
- Patla AE, Prentice SD, Robinson C, Neufeld J: Visual control of locomotion: strategies for changing direction and for going over obstacles. *Journal of Experimental Psychology: Human Perception and Performance* 1991;17:603.
- Pearson K, Ekeberg Ö, Büschges A: Assessing sensory function in locomotor systems using neuro-mechanical simulations. *Trends in neurosciences* 2006;29:625-631.
- Peterka RJ: Postural control model interpretation of stabilogram diffusion analysis. *Biological cybernetics* 2000;82:335-343.
- Seipel JE, Holmes P: Running in three dimensions: Analysis of a point-mass sprung-leg model. *The International Journal of Robotics Research* 2005;24:657-674.
- Song S, Geyer H: Regulating speed and generating large speed transitions in a neuromuscular human walking model; in: *Robotics and Automation (ICRA), 2012 IEEE International Conference on. IEEE, 2012, pp 511-516.*
- Song S, Geyer H: A neural circuitry that emphasizes spinal feedback generates diverse behaviours of human locomotion. *The Journal of physiology* 2015;593:3493-3511.
- Srinivasan M, Ruina A: Computer optimization of a minimal biped model discovers walking and running. *Nature* 2006;439:72-75.
- Taga G: A model of the neuro-musculo-skeletal system for human locomotion. *Biological cybernetics* 1995;73:97-111.
- Taga G, Yamaguchi Y, Shimizu H: Self-organized control of bipedal locomotion by neural oscillators in unpredictable environment. *Biological cybernetics* 1991;65:147-159.
- Terrier P, Dériaz O: Kinematic variability, fractal dynamics and local dynamic stability of treadmill walking. *Journal of neuroengineering and rehabilitation* 2011;8:12.
- Todorov E: Optimality principles in sensorimotor control. *Nature neuroscience* 2004;7:907-915.
- Wereley NM: Analysis and control of linear periodically time varying systems; in., *Massachusetts Institute of Technology, 1990.*
- Winfree AT: *The geometry of biological time*, Springer Science & Business Media, 2001.
- Winter DA: Human balance and posture control during standing and walking. *Gait & posture* 1995;3:193-214.
- Yang J, Stein R, James K: Contribution of peripheral afferents to the activation of the soleus muscle during walking in humans. *Experimental Brain Research* 1991;87:679-687.